Voltage-Gated Proton Channels

Thomas E. DeCoursey[*1]

ABSTRACT

Voltage-gated proton channels, H_V1, have vaulted from the realm of the esoteric into the forefront of a central question facing ion channel biophysicists, namely, the mechanism by which voltage-dependent gating occurs. This transformation is the result of several factors. Identification of the gene in 2006 revealed that proton channels are homologues of the voltage-sensing domain of most other voltage-gated ion channels. Unique, or at least eccentric, properties of proton channels include dimeric architecture with dual conduction pathways, perfect proton selectivity, a single-channel conductance approximately 10^3 times smaller than most ion channels, voltage-dependent gating that is strongly modulated by the pH gradient, ΔpH, and potent inhibition by Zn^{2+} (in many species) but an absence of other potent inhibitors. The recent identification of H_V1 in three unicellular marine plankton species has dramatically expanded the phylogenetic family tree. Interest in proton channels in their own right has increased as important physiological roles have been identified in many cells. Proton channels trigger the bioluminescent flash of dinoflagellates, facilitate calcification by coccolithophores, regulate pH-dependent processes in eggs and sperm during fertilization, secrete acid to control the pH of airway fluids, facilitate histamine secretion by basophils, and play a signaling role in facilitating B-cell receptor mediated responses in B-lymphocytes. The most elaborate and best-established functions occur in phagocytes, where proton channels optimize the activity of NADPH oxidase, an important producer of reactive oxygen species. Proton efflux mediated by H_V1 balances the charge translocated across the membrane by electrons through NADPH oxidase, minimizes changes in cytoplasmic and phagosomal pH, limits osmotic swelling of the phagosome, and provides substrate H^+ for the production of H_2O_2 and HOCl, reactive oxygen species crucial to killing pathogens. © 2012 American Physiological Society. *Compr Physiol* 2:1355-1385, 2012.

Introduction

Proton pathways through proteins are a stalwart element in numerous bioenergetic molecules, in which proton and electron movements are elaborately choreographed (27,177,269,272). In these molecules, protons generally cross partway through the membrane, perform some function, or await a catalytic step, and then return or continue across the membrane. In contrast, the voltage-gated proton channel behaves like a simple, passive conduction pathway that spans the entire membrane. Like all biological channels, proton channels are gated; that is, the channel opens to conduct protons when required, and then closes. They are called "voltage-gated" because membrane potential regulates the probability that the channel will be open, with depolarization promoting opening.

Voltage-gated proton channels are attractive subjects of research for three broad reasons. First, there is a rapidly expanding list of important physiological roles played by voltage-gated proton channels in a variety of cells and species. Second, by virtue of their homology to the voltage-sensing domains (VSDs) of other voltage-gated ion channels, they provide a unique device for evaluating gating mechanisms. Third, they violate so many rules adhered to by other ion channels that they require a new vision and a whole new set of questions. Their characterization as ion channels has occasionally been questioned on several grounds, but by most criteria, they are unquestionably ion channels. This review will summarize current knowledge in these three areas, with an emphasis on their physiological roles.

History

The first explicit proposal of a voltage-gated proton channel by Woody Hastings and colleagues in 1972 (96), postulated a role for the proton channel in triggering a bioluminescent light flash in a dinoflagellate, *Gonyaulax polyedra*, when the cell is mechanically disturbed (Fig. 1). Further information on proton channels in dinoflagellates is presented later (see Section "Bioluminescence and other functions in dinoflagellates").

Proton channels were identified as *bona fide* ion channels in 1982 by Roger Thomas and Bob Meech (260) who performed voltage-clamp studies of *Helix aspersa* snail neurons that had been impaled by a battery of microelectrodes. Protons in the form of HCl were injected into the cell bodies and outward membrane current carried by protons could

[*]Correspondence to tdecours@rush.edu

[1]Department of Molecular Biophysics and Physiology, Rush University Medical Center, Chicago, Illinois

Published online, April 2012 (*comprehensivephysiology.com*)

DOI: 10.1002/cphy.c100071

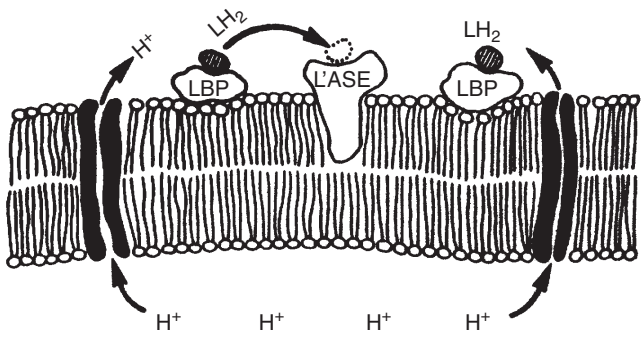

Figure 1 Voltage-gated proton channels trigger the bioluminescent light flash in dinoflagellates. The proton concentration is high in the flotation vacuole (below the membrane in the diagram). An action potential depolarizes the membrane, opening proton channels, allowing protons to flow down their electrochemical gradient into the interior of the scintillon (upper compartment). The sudden drop in pH in the scintillon triggers the flash by two concerted mechanisms. Upon protonation, the light-emitting pigment, luciferin (LH_2) is released from luciferin-binding protein (LBP) making it available as a substrate for luciferase, which is itself activated by acidification. [Adapted, with permission, from reference (109). Originally published in *Bioluminescence in Action*, edited by P. Herring, Academic Press, London. pp. 129-170, 1978. Copyright Elsevier.]

be detected when the membrane potential was clamped to positive voltages. During sustained depolarization, the outward current declined as the intracellular pH (pH_i) increased. Despite the small single-channel conductance (see Section "Minuscule single channel conductance"), proton channels were sufficiently abundant in the membrane that their activity restored pH_i on a time scale of tens of minutes. These neurons were 100 to 200 μm in diameter (56); in small cells like leukocytes (6-10 μm diameter) proton current can restore pH_i after an acid load in tens of seconds (62, 76, 134), because of the more favorable surface/volume ratio. A thorough voltage-clamp characterization carried out by Lou Byerly, Bob Meech, and Bill Moody demonstrated a critical shift of the position of the g_H-V relationship along the voltage axis when either pH_o or pH_i was changed (29). Also at UCLA, Mike Barish and Christiane Baud identified and characterized similar proton currents in *Ambystoma* salamander oocytes (19). Substantial effort was expended in these early studies to establish convincingly that proton channels were genuine ion channels and that protons did not simply permeate other channels adventitiously (29, 170). Polyvalent cations were found to inhibit proton currents (260), and Martyn Mahaut-Smith (166) showed that Zn^{2+} inhibited proton currents 80 times more potently than Ca^{2+} currents in *Helix* neurons. Byerly and Suen (30) studied current fluctuations in membrane patches from *Lymnaea stagnalis*, and concluded that the single-channel proton conductance was extremely small (< 50 fS). Based on measurements of pH changes and membrane potential, Lydia Henderson, Brian Chappell, and Owen Jones deduced the probable existence of proton channels in human neutrophils, where they were proposed to compensate for the electrogenic activity of NADPH oxidase (Nox) (115, 116).

Nearly a decade after the first voltage-clamp study, proton currents were discovered in mammalian cells, rat alveolar epithelial cells (54). These cells exhibit high levels of proton current, enabling a series of studies in which the main biophysical properties of proton channels were explored. The H^+ current was not much larger with 100 mmol/L buffer than with 10 mmol/L or even 1 mmol/L buffer, suggesting that the rate-determining step in permeation was not proton transfer from buffer to the channel, but occurred within the conduction pathway (64). Buffer concentration on the intracellular side of the membrane was, reasonably enough, shown to be important, with 100 mmol/L buffer providing markedly better control of pH_i than 10 mmol/L (64). Several studies explored the phenomenon of proton depletion as an inevitable consequence of the passage of large proton currents across cell membranes. It became clear that the proton channel does not inactivate, but that when proton depletion is pronounced, the currents decay with time as pH_i increases (54, 76, 105, 134, 184, 186). In the classical sense, "inactivation" means that a channel enters an altered conformational state from which it cannot open until recovery to a resting state has occurred (121). That proton current decay reflects changes in pH, and consequently in both the driving force and the pH-dependent gating of the channel is clear from studies showing that—whether assessed by pH electrode, pH sensing fluorescent dyes, or by measurement of the proton current reversal potential—pH_i changes roughly in proportion to the integral of the H^+ flux during pulses (54, 62, 76, 105, 134, 144, 170, 186, 260). Separating the effects of proton depletion from "genuine" underlying proton current kinetics continues to challenge researchers in this field. However, because no proton channel has yet been shown to inactivate, it remains true that visible decay of proton currents constitutes *prima facie* evidence that significant pH changes occurred during the pulse.

In 1993, proton currents were recorded in three human cell types (24, 76), including human neutrophils (60), confirming the hypothesis of Henderson and colleagues. The number of cell types reported to express proton channels continued to expand. A breakthrough in physiological function was the discovery that in phagocytes with active Nox, the properties of the proton conductance differed markedly from those in resting cells (16). The change was so profound (see Section "Enhanced gating mode") that it was at first thought to reflect the appearance of a novel type of proton channel, which was hypothesized to comprise the $gp91^{phox}$ component of the NADPH oxidase complex. First proposed explicitly in 1995 (112, 117, 118), this hypothesis gained momentum as additional members of the Nox family of proteins were discovered, and added to the list of putative dual function molecules that could alternatively transport electrons and protons (14, 15, 169). However, evidence against this hypothesis accumulated as well, as neutrophils from chronic granulomatous disease (CGD) patients who lacked functional $gp91^{phox}$ protein were shown to have normal proton currents in both resting (204) and stimulated states (69). The phorbol ester activator of protein kinase C (PKC), PMA (phorbol myristate

acetate), was shown to increase proton currents identically in PLB-985 cells with or without gp91^{phox} (69). COS-7 cells that lacked endogenous proton currents still lacked detectable proton current when gp91^{phox} was transfected into them together with other components to produce a functional NADPH oxidase complex (181). The *coup de grâce* for the hypothesis was the demonstration that neutrophils from proton channel (*HVCN1*) knockout mice exhibited no detectable proton currents, yet had normal electron currents when Nox was activated, unambiguously demonstrating the presence of functioning gp91^{phox} in their membranes (88, 178). Ironically, in their first landmark paper that proposed the existence of voltage-gated proton channels in human neutrophils (114), Henderson and colleagues made six extremely accurate predictions that remain true today:

> *"H^+ ions—movement is via a channel in the membrane, the opening of which lags behind activation of the [NADPH] oxidase. The mechanism for initiating the opening of this channel is unknown at present, but it could be a voltage decrease (i.e., depolarization), an increase in the internal concentration of protons or a phosphorylation/conformational change."*

If this had been the last word on the subject, a decade of controversy could have been avoided.

The discovery of proton channel genes in 2006 (224, 234) inevitably fomented research into several areas previously not possible, namely, structure-function studies, as well as knockout and knockdown studies, and the development of antibodies. Completely unexpected was that the proton channel molecule would so closely resemble the voltage-sensing domain of most voltage-gated ion channels. Discovery of this feature immediately transformed the proton channel molecule into a new playground for the study of voltage-gating mechanisms. In the resulting flurry of activity, discoveries have been made at an astonishing pace.

Properties

Gene and molecular features

The proton channel protein, H_V1

Identification of proton channel genes in human (224), mouse, and *Ciona intestinalis* (sea squirt) (234) in 2006 revealed surprising properties, the most remarkable of which is the similarity of the H_V1 protein to the VSD of most voltage-gated ion channels (Fig. 2). The first VSD to be identified that was not part of a voltage-gated ion channel was a voltage-sensing phosphatase (VSP) (191). The VSP senses membrane potential and exhibits "gating currents" like those associated with voltage-gated ion channels, but the response to depolarization is modulation (an increase) of phosphatase activity. The subsequent identification of the voltage-gated proton channel gene added impetus to the idea that the VSD might be viewed as a modular unit that could be attached to another molecule and provide voltage sensitivity to its function (143, 173, 176, 207). The Swartz group have further shown that the "paddle motif" (the S3b and S4 transmembrane helices)

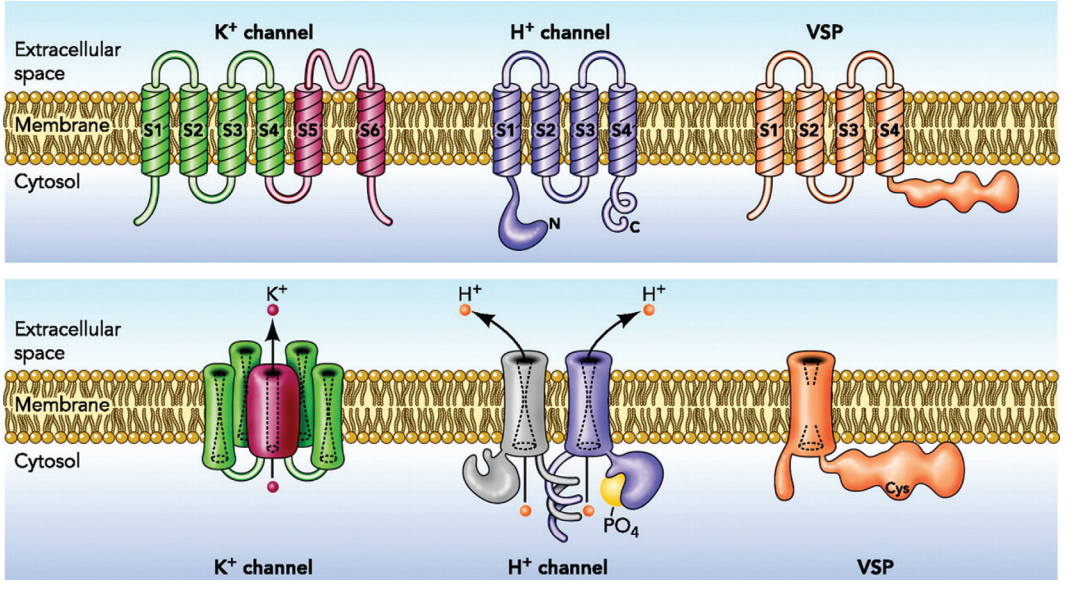

Figure 2 Membrane topology of voltage-gated K^+ channels (left), voltage-gated proton channels (center), and voltage-sensitive phosphatases (right). The K^+ channel (lower panel) is a tetramer of the six transmembrane domain monomer shown in the top; the proton channel is a homodimer of the four transmembrane domain monomer in the top panel, and the phosphatase is a monomer. The assembled K^+ channel has a single conduction pathway, but the proton channel has two, one in each protomer. The voltage-sensing phosphatase (VSP) senses voltage, but does not conduct. The proton channel cartoon illustrates schematically that the dimer is held together by C-terminal coiled-coil interactions, and that the channel can be phosphorylated at Thr^{29} in the intracellular N terminus to produce the enhanced gating mode (cf. Figure 20). [Figure adapted, with permission, from reference (58). Originally published in *Physiology* 25:27-40, 2010.]

is indeed modular, and continues to function when swapped among K^+ channels, H_V1, and VSP (7).

Perhaps, the most distinctive feature of the proton channel is the absence of S5-S6 domains that form the conduction pathway in ordinary ion channels. Because conduction can be demonstrated when purified H_V1 protein is reconstituted in synthetic liposomes, no accessory protein is required (151). The conduction pathway must exist within the H_V1 molecule itself. Homology models have been proposed, based on the similarity of the sequence to that of the VSD of K^+ channels (199,223,270). The channel resembles an hourglass filled with water, with a constriction near the center. Proton selectivity is established by an essential aspartate residue in the S1 domain, Asp^{112} in hH_V1 (200) and Asp^{51} in kH_V1 (251), which is thought to be located at or near the constriction when the channel is in the open state.

Three new proton channel genes were discovered in 2010, all in unicellular marine organisms; two coccolithophores, *Emiliania huxleyi* and *Coccolithus pelagicus* (259) and a dinoflagellate, *Karlodinium veneficum* (251). These channels greatly expand the phylogenetic representation of H_V1 (Fig. 3). One putative plant H_V1 is shown. Only seven of the 37 putative *H_V1* genes have been confirmed by heterologous expression and electrophysiological recording; in addition to the six just discussed, *Strongylocentrotus purpuratus* was confirmed by Y. Okamura (personal communication). The confirmation that H_V1s in several unicellular species are genuine proton channels is an important validation of the criteria used to identify putative proton channels from sequence analysis alone. We proposed recently that a protein with four transmembrane domains that includes (a) an appropriately positioned Asp residue in S1 to act as the selectivity filter and (b) two or preferably three appropriately spaced Arg residues in

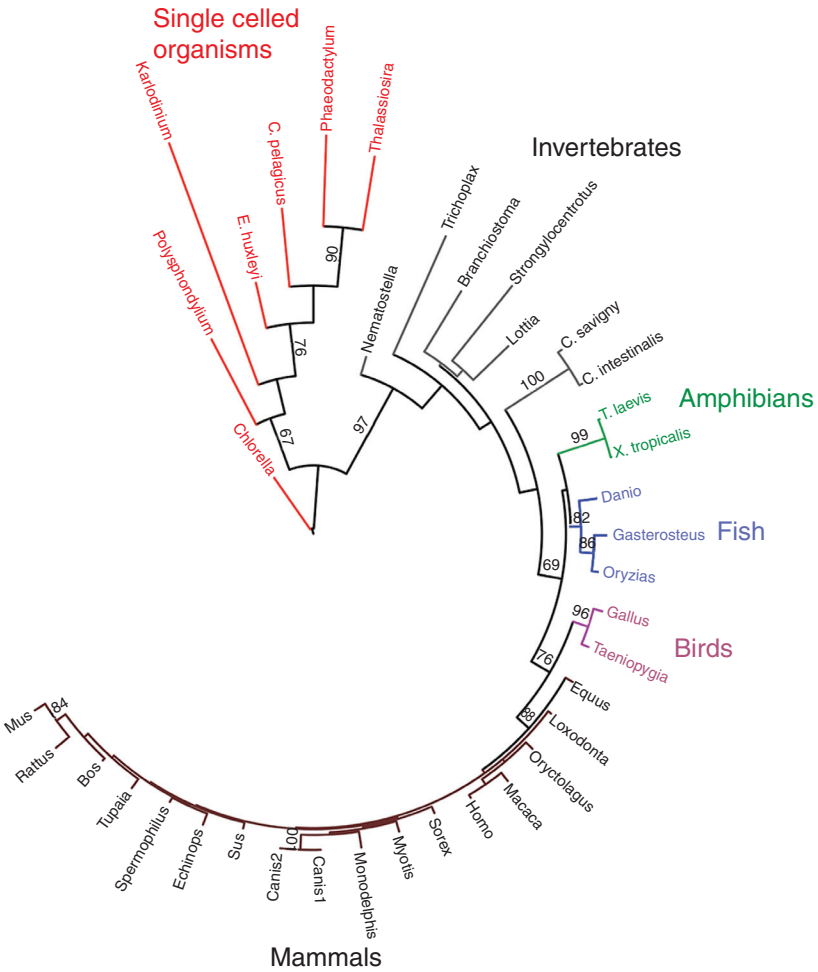

Figure 3 A phylogenetic analysis showing evolutionary relationships among 37 putative H_V1 voltage-sensing domain (VSD) sequences. This maximum likelihood phylogenetic tree with 100 boostraps was constructed from a multiple sequence alignment of the VSD portion of 37 H_V1s; N- and C-termini were truncated. Branch lengths are displayed to scale, and are proportional to the evolutionary distance between sequences. Bootstrap values greater than 60 are shown. [Figure adapted, with permission, from reference (251). Originally published in *Proc. Natl. Acad. Sci. U S A.* 108:18162-18168, 2011.].

S4, that include the WRxxR motif, can be considered highly likely to be a voltage-gated proton channel (251).

The phylogenetic tree in Figure 3 is drawn to scale, so that the radial length of each branch reflects the extent of sequence differences. It is tempting to overinterpret this phylogram. Mammalian H_V1s are very similar to each other, but as one ventures toward more primordial species, variation increases. Invertebrate H_V1s exhibit a high degree of individuality, and H_V1s in unicellular organisms are riotously diverse. The most deviant among this group is kH_V1, a dinoflagellate proton channel. One might predict that in general, sequence diversity may presage functional diversity. As we will discuss later (see Section "Bioluminescence and other functions in dinoflagellates"), the *Karlodinium* proton channel violates the hitherto sacred rule of conducting exclusively outward current (251), and thus its unique behavior matches its idiosyncratic sequence.

Nomenclature

The discoverers of the first proton channel genes adopted different systems for nomenclature. Ramsey and colleagues (224) christened the human channel H_V1: H for H^+ selective, V for voltage-gated, and 1 for its being the first example identified in humans. Sasaki and colleagues adopted more evocative abbreviations, mVSOP and CiVSOP: m for mouse, Ci for *C. intestinalis*, and VSOP for voltage-sensor-only protein (234), thus incorporating the most surprising feature of the gene product into its designation. The official gene name for all species is *HVCN1*. Here, I will adopt the more austere convention and refer to the protein as H_V1, which will be qualified by a prefix that indicates species (hH_V1 for human, mH_V1 for mouse, etc.). Although this appears to limit the spectrum to 26 species (and then only if they have different initials), the list can be expanded by including genus and species, for example, CiH_V1, EhH_V1, or CpH_V1. To date, only one proton channel gene has been identified in any species, so for now, the suffix is 1 for all species.

The proton channel is a dimer, exhibiting cooperative gating

Several types of evidence led to the conclusion that the proton channel molecule exists mainly as a dimer, both in heterologous expression systems (139, 150, 261) and in native cells (217), with a conduction pathway in each protomer (139, 261). It is puzzling why the channel goes to the trouble of assembling as a dimer, in light of evidence that the monomer exhibits the main features of native proton current: activation upon depolarization, extreme proton selectivity, and exquisite sensitivity of gating to both pH_o and pH_i (103, 139, 199, 261). A precedent exists for a dimeric channel with conduction pathways in each monomer, in the ClC family of Cl^- channels and Cl^-/H^+ antiporters (1, 108, 159, 163, 171, 172, 174). Like ClC-0 (108), the two protomers comprising the proton channel dimer appear to interact during gating (103, 198, 199, 262). This interaction has been interpreted either as positive cooperativity in which the opening of a single protomer greatly increases the probability of the second protomer opening (262), or a strict requirement that both protomers undergo a conformational change before either can conduct (103, 198, 199). Coiled coil interactions at the C terminus appear to provide the main glue that holds the dimer together (103, 139, 151, 156, 198, 199, 261). Truncating (or replacing) the C terminus results in expression of monomers (103, 139, 198, 199, 261) that open 5-6 times more rapidly than the wild-type (WT) dimer (139, 198, 261). As illustrated in Figure 4, the proton conductance of the dimer activates with a sigmoid time course, consistent with classical Hodgkin-Huxley n^2 kinetics (122), whereas the monomer activates exponentially (103, 199). Figure 4C shows that during depolarizing pulses a fluorescent probe attached to the S4 domain moves with an exponential time course, whereas the current turns on after a small delay and with a sigmoid time course. Reflecting the cooperativity of gating, the limiting slope of the g_H-V relationship of the dimer is twice as steep as that of the monomer (103). These properties of dimeric gating suggest an explanation for the utility of proton channels existing as dimers, at least in phagocytes (199). As will be seen (see Section "Charge compensation"), proton channels open in phagocytes to prevent excessive depolarization caused by the electrogenic activity of Nox. Consequently, it is critically important that proton channels activate with a steep voltage dependence, to prevent self-inhibition of Nox (73). If steep voltage dependence occurs at the expense of slower opening, little is lost. Depending on the type of stimulus, the time course of the respiratory burst is relatively slow, usually preceded by a delay of seconds to minutes, and persisting for minutes to hours (72).

The dimeric arrangement may not dictate an invariant interface. Two possible interfaces have been proposed, shown in Figure 5. On the basis of cross-linking studies for mutants in which Cys was introduced at various locations in the hH_V1 molecule, several interactions at the external end of S1 (shown in red in Fig. 5A) were detected (150). However, based on Zn^{2+} effects on hH_V1 mutants in which the Zn^{2+}-binding residues His^{140} and His^{193} were mutated, the interface shown in Figure 5B was proposed to occur at least occasionally (199). In the Cys scanning study, weak cross-links were observed at position 194, right next to His^{193}, suggesting that this orientation can occur at least occasionally (150). If both kinds of interfaces are possible, then multimers could also occur (Fig. 5C). Given substantial evidence that the protomers interact during gating, one imagines that channel opening might occur only from a particular orientation. Because Zn^{2+} appears to prevent channel opening (36), it is reasonable to suppose that Zn^{2+}—which is thought to bind at the interface between protomers (199)—might act by preventing the dimer from adopting its preferred orientation.

Although the dimer is normally stabilized by C terminal coiled-coil interactions (150, 156, 261), a tandem dimer in which the C terminus of one protomer was connected by a

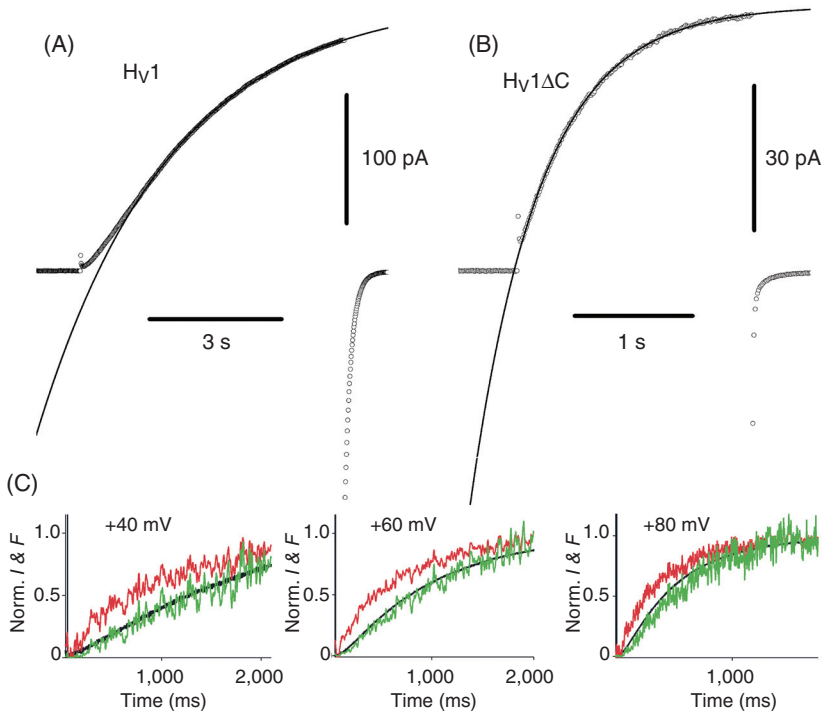

Figure 4 Comparison of gating kinetics of the human proton channel dimer (A) and monomer (B), expressed in HEK-293 cells. Note the slower, sigmoid activation of the WT channel (A), and the faster, exponential turn-on of the monomer (C terminus truncated, $H_V1\Delta C$) both during pulses to +50 mV at 23°C at pH_o 7.5, pH_i 7.5. [Adapted from reference (199). Originally published in The Journal of Physiology.] (C) The time course of movement of a fluorescent probe attached to the S4 domain of the *Ciona* proton channel is exponential (red). This time course raised to the second power (green) matches the proton current recorded at the same time (black). [Adapted, with permission, from reference (103). Adapted, with permission, from Macmillan Publishers Ltd: *Nature Structural & Molecular Biology* 17: 51-56, 2010.]

short linker to the N terminus of the second protomer functioned almost identically to the WT dimer (198, 199). The tandem dimer activated with a sigmoid time course (198), consistent with similar cooperative interactions between protomers observed in WT dimers (103). Its g_H-V relationship was also indistinguishable from WT, and the only difference detected was slower activation kinetics (198). Evidently, C terminal coiled-coil interactions tether the two protomers together, but appear not to contribute critically to the interactions between protomers that occur during channel gating (198). However, a role of the C terminus in modulating gating by direct mechanical linkage has been suggested (99).

In contrast to the structural role played by the C terminus, the N terminus appears to interact closely with the gating mechanism of the channel. The enhanced gating mode (see Section "Enhanced gating mode") is mainly the result of phosphorylation of Thr^{29} in the N terminus of hH_V1 (194). In addition, a mutation that results in M91T substitution (Met replaces Thr at position 91) in the N terminus has been identified in the human population (128) (see Section "Acid secretion in epithelia of the respiratory tract"). This mutation shifts the g_H-V relationship positively by 20 mV, reducing the likelihood of channel opening. It remains unclear how these two residues scattered among the 100-residue N terminus of hH_V1 are able to modulate gating, which as discussed previously presumably involves movement of the S4 domain relative to the other transmembrane domains.

Selectivity and permeation by protons

Perfect selectivity

The voltage-gated proton channel appears to be perfectly selective, or specific, for protons. At present, no evidence even suggests that any other ion can permeate. Numerous studies in many cell types have demonstrated that when the dominant cation or anion in the bathing solution is changed, the measured reversal potential (V_{rev}) does not change, after liquid junction potentials are corrected (56, 58, 200). Any small deviation of V_{rev} from the Nernst potential for protons (E_H), is therefore attributable to imperfect control of pH. Even if the entire discrepancy between V_{rev} and E_H were due to permeation of other ions through the channel, the relative permeability for protons over other ions is greater than 10^6 when calculated with the Goldman-Hodgkin-Katz equation (102, 119, 123). How can such a high degree of proton selectivity be achieved?

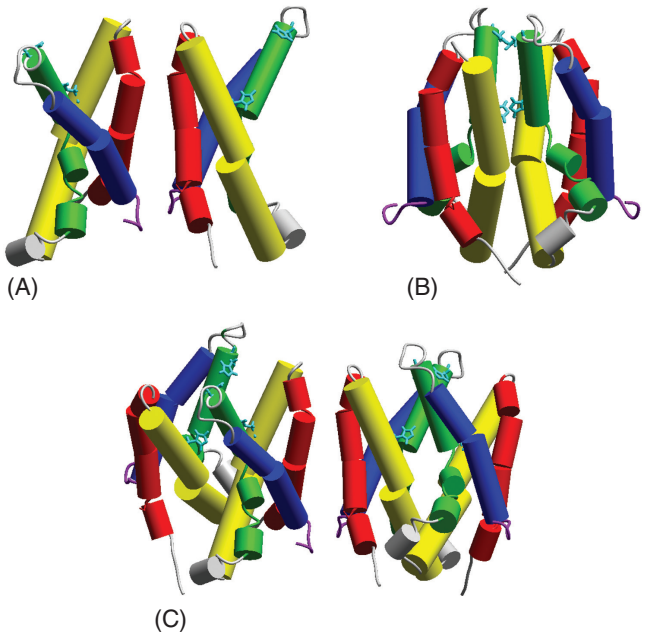

Figure 5 Possible dimer interfaces, with the transmembrane domains color coded as: S1 red, S2 yellow, S3 green, and S4 blue. The dimer in A was proposed on the basis of cysteine cross-linking studies (150); the dimer in B was proposed to explain Zn^{2+} binding studies (199). External His residues that bind Zn^{2+} (224) are shown in aqua (cf. Figure 14). [Adapted, with permission, from reference (198). Originally published in Channels (Austin) 4: 260-265, 2010.]

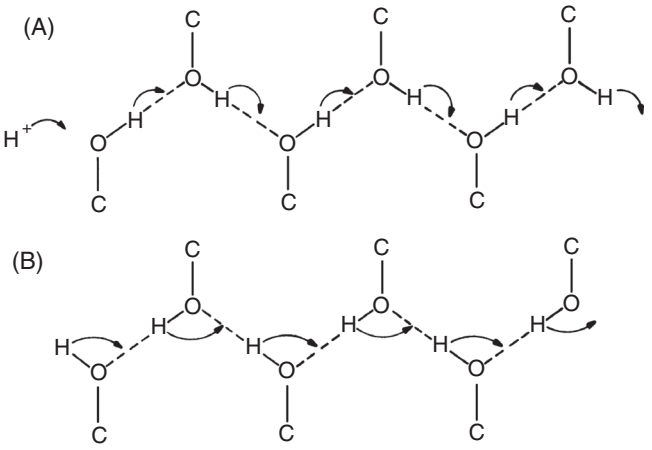

Figure 6 Hydrogen-bonded chain (HBC) conduction. In this schematic example, hydroxyl groups (e.g., from Ser residues) form a HBC that spans the membrane. (A) Proton conduction occurs when a proton enters the chain from the left to form a positive ion, which then moves to the right by hopping of successive protons to effect a reversal of the direction of the hydrogen bonds between each pair of oxygen atoms. Proton conduction would also occur by loss of a proton on the right followed by movement of a negative ion (or fault) to the left. (B) To complete the process, reorientation of each hydrogen bond in the chain must occur, so that another proton can enter from the same side. [Redrawn, with permission, from reference (202).]

Proton conduction through proteins is widespread, appears to occur fairly readily, and is presumed to be possible whenever water molecules are identified inside proteins within hydrogen bonding distance of other waters or titratable groups. Many membrane proteins have been shown to be capable of conducting protons, several of which were discussed previously in this context (56). However, despite the apparent facility of proton conduction, proton *selective* conduction is more demanding, and is discussed later. It is arguably more difficult to prevent protons from carrying current through an aqueous pathway, than to allow proton permeation. This challenge is faced by aquaporins, whose job is to facilitate rapid water permeation (4), but to prevent permeation by ions, especially protons. Precisely how protons are excluded remains debatable (28, 33, 51, 127, 175, 190, 256). Intriguingly, mutation of just three amino acids turns AQP1 into a cation-conducting channel with a strong preference for protons (273).

Protons are chemically quite different from other cations. In aqueous solutions, protons exist as H_3O^+ at least 99% of the time (47). By hopping from one water molecule to the next by the Grotthuss mechanism (3, 49, 52, 53), proton conduction through water occurs five times more rapidly than other cations the same size as H_3O^+ (23, 86). Proton conduction through proteins occurs by a hydrogen-bonded chain (HBC) mechanism (202) in which protons hop from one molecule or group to the next (Fig. 6). The HBC may comprise titratable amino acid side chains or water molecules (202). Because protons are ubiquitous (the total concentration of hydrogen in water is 110 mol/L) and interchangeable, multiple protons contribute to the net flux of a single proton across the membrane. Other ions diffuse around water and other molecules; protons use water and other molecules as stepping stones. The HBC mechanism potentially enables proton selective conduction, by virtue of the ability of protons to translocate along the chain without displacing the elements of the chain. Thus, protons are conducted through the gramicidin channel, which contains a linear row of a dozen water molecules (154), two orders of magnitude faster than any other ion (201), because other ions must wait for the waters to diffuse through the pore. The protons hop across, leaving the water wire intact.

Compared with proton conduction through the gramicidin channel, which is viewed as an archetypal water-filled pore, conduction through voltage-gated proton channels seems distinctly more challenging. The mobility of protons within gramicidin is roughly comparable to that in bulk water scaled to channel-like dimensions (48). In contrast, proton permeation through voltage-gated proton channels has a much higher deuterium isotope effect: $g_H/g_D = 1.9$ for proton channels (66) versus 1.35 for gramicidin (6, 42). In addition, the temperature dependence for proton permeation through voltage-gated proton channels is 12 to 27 kcal/mol (67, 144) versus 3 to 8 kcal/mol for proton permeation through gramicidin (6, 41). The strong isotope effect and temperature sensitivity can be explained if protons permeate via a HBC comprising titratable amino acid side chains in addition to water. Given these properties in addition to the extreme selectivity of the voltage-gated proton channel, and the indication from buffer effects that the rate-limiting step in H^+

permeation occurred in the pore (64), the general opinion was that the permeation pathway through voltage-gated proton channels likely contained at least one titratable group (56,61,62,66,67,77,117,169). Recently, this hypothesis was tested by mutating every likely HBC element in the human H_V1 proton channel (223). No single residue was found to be indispensable for conduction. By default, the mechanism of proton selectivity was suggested instead to involve non-diffusible waters "frozen" at a narrow constriction in the channel. These waters could transfer H^+ but block permeation of ordinary ions. Even more recently, Asp^{112} located in the S1 TM domain was identified as the proton selectivity filter of the human voltage-gated proton channel (200). Neutralizing mutations not only eliminated proton specific conduction, they resulted in permeability to anions. The conservative replacement of Asp with Glu did not alter proton selectivity, but the D112H mutant was anion permeable. The corresponding residue in a dinoflagellate proton channel, Asp^{51}, also in the S1 domain, was found to exhibit identical phenomenology; neutral substituents produced a strongly Cl^- permeable channel, Glu acted like Asp, and the His mutant conducted Cl^- (251). Evidently, when the Asp at the selectivity filter is neutralized, the rest of the channel molecule excludes cations. How proton-specific conduction is enforced is not yet understood in atomic detail, but an acid at this key location in the first transmembrane domain (S1) is essential.

A similar problem has been confronted by the M_2 proton channel of influenza A virus. This channel shares many biophysical properties with the voltage-gated proton channel, including high selectivity (43, 158, 189), small conductance (158, 189), and a large deuterium isotope effect (189). However, surprising new studies indicate that the M_2 channel is not exclusively proton selective, but that Na^+ and K^+ can occasionally permeate in the opposite direction, compensating electrically for H^+ influx (152, 215). If M_2 is less selective than the voltage-gated proton channel, then its direct relevance as a model for the selectivity mechanism of the voltage-gated proton channel may be questioned, but it remains heuristically useful. The M_2 channel is a homotetramer with a ring of four His^{37} residues that comprise an acid-activated gate. One conceptual model postulates that protonation of these His^{37}, through electrostatic repulsion, expands the channel allowing waters to transfer protons down the center of the pore while still preventing other cations from permeating by a frozen water mechanism (136,142,233,252). Alternatively, His^{37} might be protonated and deprotonated with each conduction event, shuttling protons through the pore (124, 137, 148, 218, 241, 245, 248). Recently, a hybrid mechanism was suggested, in which the permeating proton is delocalized among the four His^{37} and associated water molecules (2). Whether a proton delocalization mechanism might also be applicable to the voltage-gated proton channel remains to be determined. The idea seems seductively vague, but it may actually reflect reality. Surprisingly, mutation of Asp^{112} in hH_V1 to His (D112H) failed to produce proton-selective conductance; instead, the D112H mutant was anion permeable (200). Precisely, the same result was seen in the D51H mutant of the dinoflagellate proton channel kH_V1 (251). Evidently, His can shuttle protons, but even at a constriction, does not guarantee proton specificity.

Minuscule single channel conductance

One of the most exciting possibilities enabled by the discovery of the patch-clamp technique was the direct measurement of current flowing through a single molecule, an open ion channel (106). Most ion channels have a conductance of 2 to 400 pS (119), and conduct currents of a few picoamperes, that are resolvable by direct recording from a patch of membrane, or even from whole cells that are electrically tight [such as human lymphocytes (59) or eosinophils (90)]. However, the voltage-gated proton channel has a conductance approximately 3 orders of magnitude smaller than most other channels, and for many years single channel currents were thought to be too small to resolve by direct measurement. Due to the difficulty in resolving single-channel currents, a preferred approach is to evaluate current fluctuations, which provides similar information, as illustrated in Figure 7. At subthreshold voltages, the current exhibits very little noise. Above threshold, the random gating of proton channels introduces noise into the current, from which the single-channel current amplitude, i_H, can be derived: $i_H = \sigma^2/[I_H \times (1\text{-}P_{open})]$, where σ^2 is the variance and P_{open} is the open probability (119). These parameters are all directly measurable, excepting P_{open}, which can be accounted for by selecting conditions that minimize its effect; by recording just above $V_{threshold}$ where $P_{open} \approx 0$ (60), or by analyzing data from multiple voltages simultaneously (39, 244). Determined in this way, the unitary conductance increased as pH_i decreased, from 38 fS at pH_i 6.5 to 140 fS at pH_i 5.5 at room temperature (39). The unitary conductance was independent of pH_o, as might be expected for exclusively outward currents. Incidentally, this behavior is consistent with H^+ being the conducted species, rather than OH^-, which would be expected to have the opposite dependence on pH changes. In some patches, Cherny and colleagues observed step-like events that resembled single-channel currents, with amplitudes 7-16 fA fluctuations (39). These were just on the boundary of being resolvable, and required seal resistances in the TΩ (10^{15} Ω) range; because at the low frequencies of proton channel gating, the resolution is limited by extraneous noise contributed by the seal resistance (153). The amplitude of these apparent unitary currents was about double that calculated in the same patches from fluctuations (39). This result is intriguing in light of the proton channel existing as a dimer (139, 150, 261), whose two subunits each have separate conduction pathways and function with strong cooperativity (103, 198, 199, 262).

Once the unitary conductance is known, it is possible to calculate the open probability of the channel, P_{open}. The limiting P_{open} for large depolarizations, P_{max}, was found to

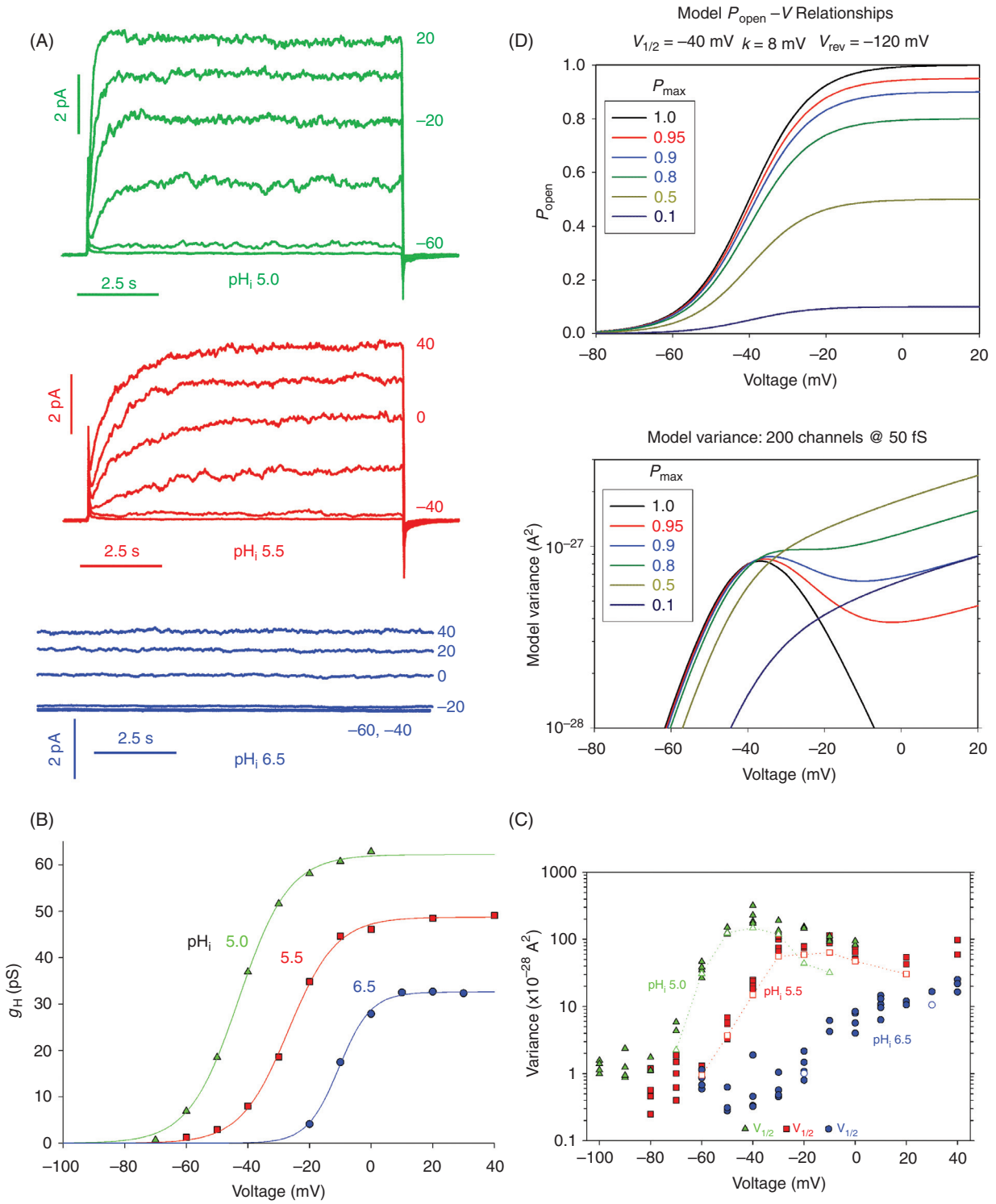

Figure 7 Determination of the single channel conductance from proton current fluctuations that reflect the stochastic opening and closing of proton channels. "A" shows families of proton currents in an excised, inside-out patch from a human eosinophil at three pH_i values. At subthreshold voltages, the current is quiet, but just above $V_{threshold}$, proton channels begin to open, and the current becomes distinctly noisy. It is noteworthy that (at low pH_i) the noise first increases with depolarization, but then decreases for large depolarizations. "B" shows g_H-V relationships from this patch. The variance of the current fluctuation, measured at quasi-steady-state, is plotted in "C." The variance increases more than 100-fold at voltages where the proton conductance is active, and is maximal near the midpoint of the g_H-V relationship at each pH_i (indicated as $V_{1/2}$). "D" shows that the expected variance given the simplest possible two-state model of gating (closed ↔ open) coincides with the observed voltage dependence. The nonmonotonic increase in variance with depolarization is consistent with the maximum P_{open} limiting to approximately 0.95 at pH_i 5.5. [Adapted, with permission, from reference (39) © Cherny et al., 2003. Originally published in The Journal of General Physiology.]

be 0.75 at pH_i 6.5, increasing to 0.95 at pH_i 5.5 or lower (39). Thus, lowering pH_i increases proton currents both by increasing the unitary conductance and by increasing P_{max}.

Regulation of gating by the pH Gradient, ΔpH

A feature displayed universally by voltage-gated proton channels is that the voltage dependence of their gating shifts drastically when pH is changed on either side of the membrane. Lowering pH_o shifts the g_H-V relationship positively and tends to slow channel opening (larger activation time constant, τ_{act}) (19, 29). Byerly and colleagues (29) observed that the slowing of activation at lower pH_o was greater than could be accounted for by the size of the g_H-V relationship shift (i.e., on the assumption that all gating parameters shifted equally), and concluded that external protons directly inhibited channel opening in snail neurons. Conversely, lowering pH_i shifts the g_H-V relationship negatively (29, 167). Figure 8 illustrates the effects of changes in pH_i on proton currents in inside-out patches of membrane from rat alveolar epithelial cells (63). Qualitatively, the effects are like those described in snail neurons, but there are subtle differences. Effects of pH_o on τ_{act} appear to be accounted for by the 40 mV/unit pH shift of the g_H-V relationship, in contrast with snail. However, lowering pH_i in rat increased the current amplitude and greatly accelerated activation. In rat epithelium, τ_{act} decreased 5-fold per unit decrease in pH_i, which cannot be ascribed to a voltage shift. These minor differences probably reflect species differences, but some subtle discrepancies seem to exist between properties observed in excised membrane patches compared with those in whole-cell configuration. Nevertheless, the qualitative effects of pH_o and pH_i are quite consistent among all species studied to date. The physiological implication of this intricate regulation by pH is that the proton channel normally conducts only outward current, and consequently, its primary function must be acid extrusion from cells.

In stark contrast to the effects of pH_o on channel activation, deactivation was completely insensitive to pH_o in human THP-1 cells (65). A weak sensitivity to pH_o was seen in rat alveolar epithelial cells if the tail currents were force-fit by a single exponential, but when a double exponential fit was used, the rapid τ_{tail} component was pH_o independent. Near $V_{threshold}$, a slower component of tail current decay appeared that was kinetically closer to τ_{act} and was more steeply voltage dependent, as well as being shifted ~approximately 40 mV/unit change in pH_o (38).

In a systematic study of the regulation of the voltage-activation curve by pH, it was discovered that increasing pH_o or decreasing pH_i by one unit shifted the g_H-V relationship by −40 mV (38), as illustrated in Figure 9A and B. This relationship was quantified as the Rule of Forty:

$$V_{threshold} = -40\ mV \times (\Delta pH) + 20\ mV \qquad (1)$$

where $V_{threshold}$ is the "threshold" voltage at which proton currents are first evident and $\Delta pH = pH_o - pH_i$. Although $V_{threshold}$ is an artificial construct, when used rationally and consistently, it is an extremely useful tool for evaluating *changes* in the position of the g_H-V relationship. A metric more in vogue for other voltage-gated channels is to fit their g-V relationship to a Boltzmann function, to obtain a slope factor and a midpoint voltage. However, for proton channels, this approach provides only the illusion of quantification. Under most experimental conditions, proton depletion combined with slow activation kinetics precludes straightforward measurement of the g_H-V relationship, so that Boltzmann parameters become meaningless (196). An alternative form of Eq. (1) that does not require precise knowledge of pH_i (which often deviates from its nominal value, even when attempts are made to control it) is:

$$V_{threshold} = 0.76 \times V_{rev} + 18\ mV \qquad (2)$$

in which V_{rev} is the measured reversal potential (66). Both Eqs. (1) and (2) were determined in rat alveolar epithelial cells. When data from all studies published by 2003 were included, encompassing 15 cell types, the result was quite similar, as illustrated in Figure 10:

$$V_{threshold} = 0.79 \times V_{rev} + 23\ mV \qquad (3)$$

The physiological meaning of this relationship, as alluded to previously, is that the proton channel evidently evolved into an ideal acid extrusion mechanism. In fact, the regulation of its gating by pH suggests that the voltage-gated proton channel was engineered to solve "the central problem of pH_i regulation: the neutralization of intracellular acid derived from a variety of sources" (228). Over a very wide range of pH_o and pH_i encompassing most or all physiological conditions, proton channels open only when there is an outward electrochemical gradient. They open only when doing so will result in outward H^+ current, that is, acid extrusion (56).

Now that we have enshrined an absolute rule, we will immediately identify an exception. A spectacular deviation from the universality of Eq. (3) was identifed recently in dinoflagellates (251). The proton channel from *K. veneficum*, kH_V1, is regulated by ΔpH with an offest of −37 mV, so that its $V_{threshold}$ is always 60 mV more negative than in other proton channels:

$$V_{threshold} = 0.79 \times V_{rev} - 37\ mV \qquad (4)$$

Figure 10 illustrates that $V_{threshold}$ data from kH_V1 (green dots) always fall below the red dashed line of equality between V_{rev} and $V_{threshold}$. The consequence is that kH_V1 conducts *inward* rather than outward H^+ current over a wide voltage range. The function of the dinoflagellate proton channel is thus clearly very different from that in all other species, and will be discussed later (see Section "Bioluminescence and other functions in dinoflagellates"). However, despite its anomalous voltage dependence, not to mention its evolutionary distance

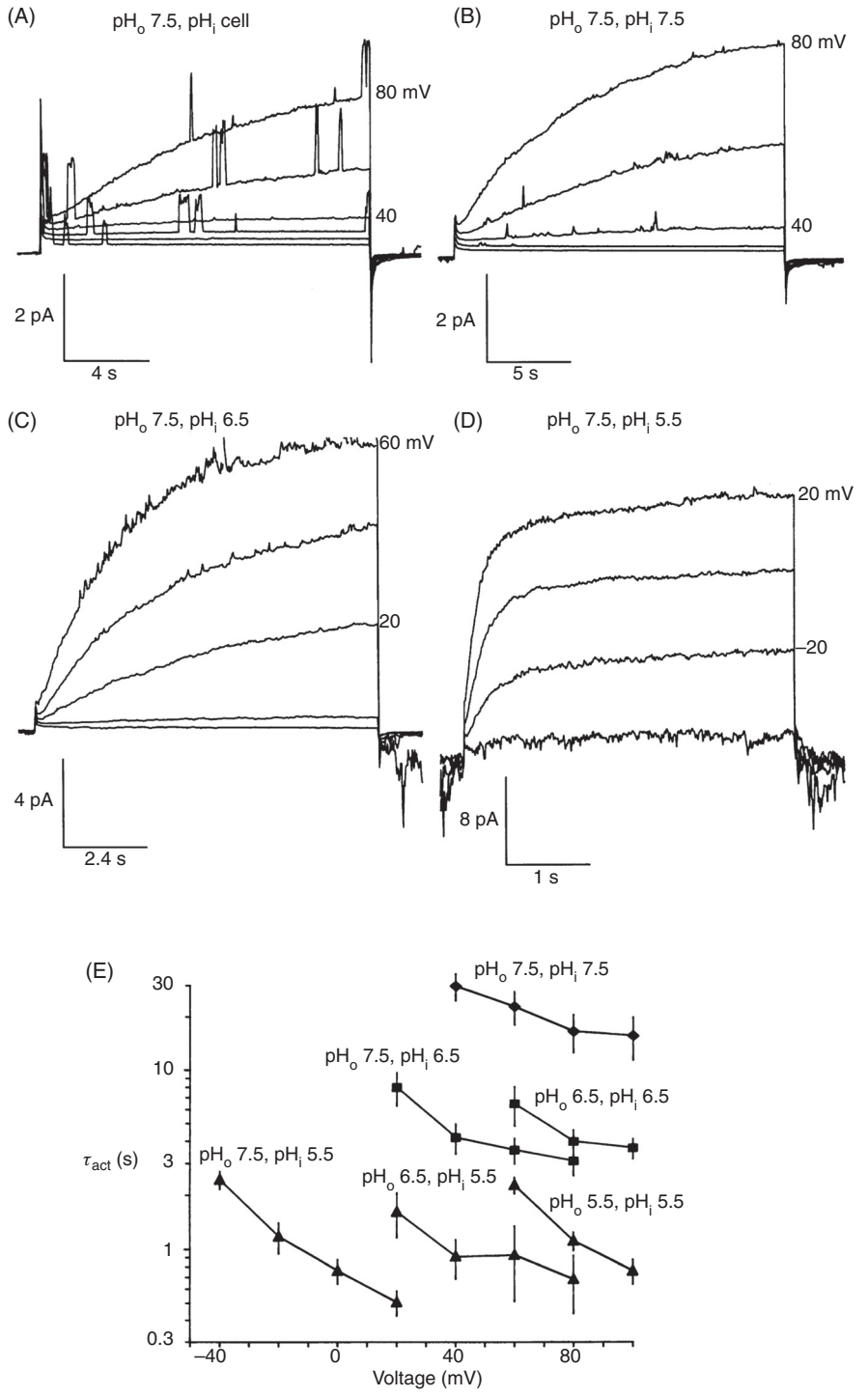

Figure 8 (A-D) Effects of pH_i on voltage-gated proton currents in an inside-out membrane patch from a rat alveolar epithelial cell. The pipette pH (i.e., pH_o) was 7.5. "A" shows proton currents in a cell-attached patch that increase gradually with time during each pulse because the single channel proton currents are too small to resolve. Superimposed are large single channel currents most likely due to Kv1.3 delayed rectifier channels that dominate macroscopic currents in these cells (71). After this patch was excised into K^+-free solutions, the same population of proton channels generated the currents shown in "B-D" at the indicated pH_i. As pH_i was decreased, the currents became larger and activated much more rapidly (note the changing calibrations). The graph in **E** shows average activation time constants (τ_{act}) obtained by single exponential fits in many patches. Changing pH_o shifts the kinetics along the voltage axis with little change in the range of τ_{act} values. In contrast, changes in pH_i profoundly affect τ_{act}, with an approximately 5-fold slowing per unit increase in pH_i. [Adapted, with permission, from reference (63). Originally published in The Journal of Physiology 489:299-307, 1995.]

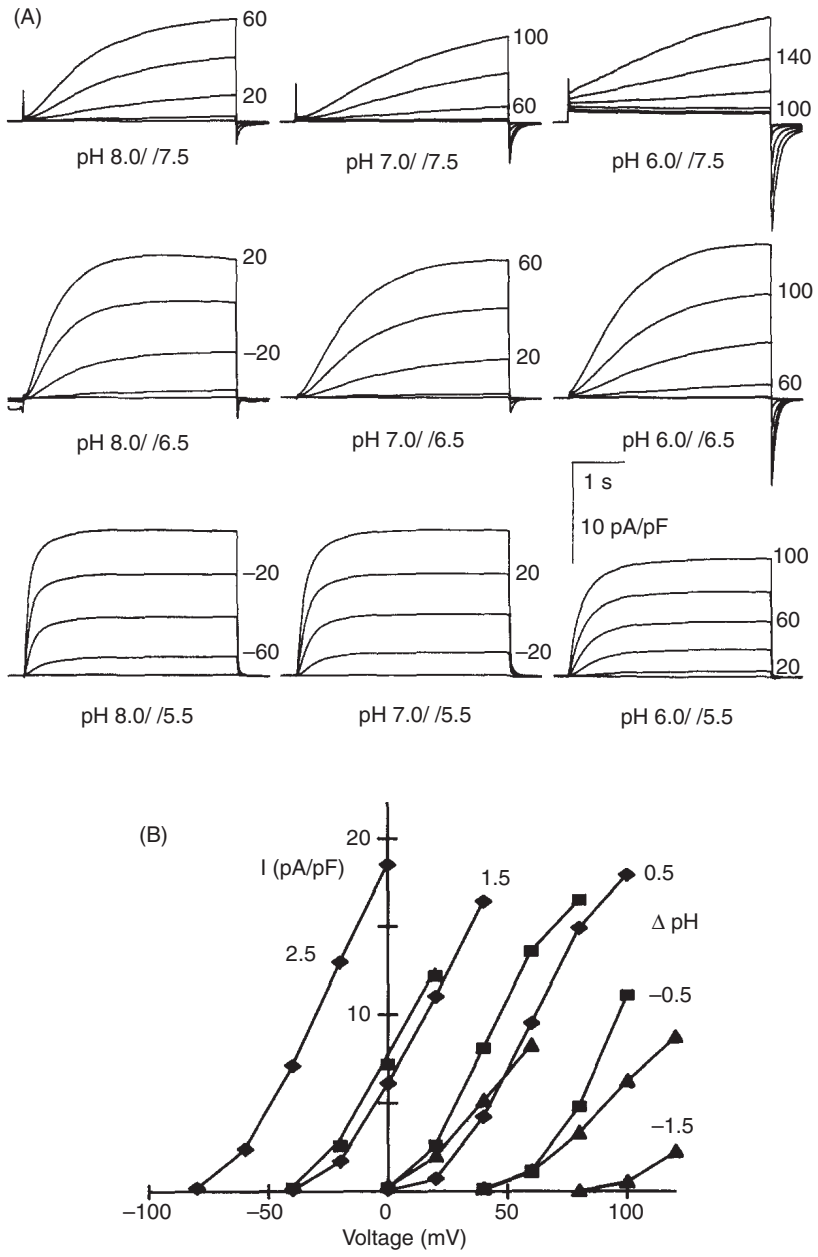

Figure 9 (A) Families of proton currents at different $pH_o//pH_i$ in three rat alveolar epithelial cells (one in each row). The most obvious effect of pH is to vary the voltage range in which proton channels open. (B) Average current-voltage relationships at the indicated ΔpH, where $\Delta pH = pH_o - pH_i$, illustrate that the position of the g_H-V relationship is completely determined by ΔpH. The "Rule of Forty" (Eqs. 1-3) expresses the 40-mV shift in the position of the g_H-V relationship that occurs when ΔpH changes by one unit, regardless of whether pH_o or pH_i is changed. [Adapted, with permission, from reference (38) © Cherny et al., 1995. Originally published in The Journal of General Physiology 105:861-896.]

from humans, it is noteworthy that kH_V1 still obeys the Rule of Forty (251). It is difficult to escape the conclusion that the gating of all voltage-gated proton channels is regulated by ΔpH by a similar mechanism. The details of this mechanism remain obscure. The possibility that a single titratable residue might govern the ΔpH dependence was eliminated by a comprehensive study in which most such groups were individually mutated to Ala or another neutral residue (223). Every mutant studied obeyed the Rule of Forty, retaining a roughly 40 mV/unit pH shift when pH was varied, although the absolute positions of the g_H-V relationships varied widely. The mechanism responsible for the pH dependence of gating is evidently subtler and substantially more robust than a simple modulatory site.

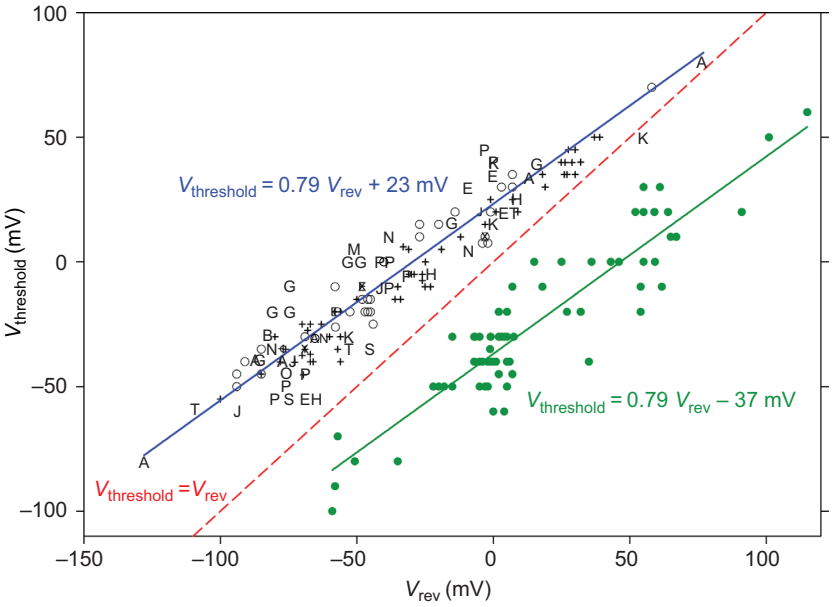

Figure 10 Regulation of the position of the g_H-V relationship by ΔpH occurs in all known voltage-gated proton channels. In most species, this regulation results in $V_{threshold}$ always being positive to the reversal potential, V_{rev}, thus ensuring that when proton channels open, acid will be extruded. The blue line shows the result of linear regression on data reported in 15 cell types that are listed in reference (56); the dashed red line shows equality between $V_{threshold}$ and V_{rev} for comparison. In the recently identified kHv1 channel in the dinoflagellate, *Karlodiniun veneficum*, $V_{threshold}$ is shifted by −60 mV relative to all other species (green data points and line), with the result that depolarization above $V_{threshold}$ will produce inward H^+ current in kH_V1 at all ΔpH (251).

Gating kinetics

Voltage-gated proton currents appear to electrophysiologists very similar to many other voltage-gated channel currents. In fact, to someone familiar with delayed rectifier K^+ currents, proton currents evoke a sense of *déjà vu*, with the exception of the time scale being orders of magnitude slower. Both currents activate sigmoidally; this appears to reflect n^2 kinetics for dimeric proton channels (103), but n^4 kinetics for tetrameric K^+ channels (122). Both H^+ and K^+ channels exhibit the Cole-Moore effect, in which the delay before the current turns on during depolarization increases with preceding hyperpolarization (46, 62). Both H^+ and K^+ currents deactivate exponentially upon repolarization, and τ_{tail} is generally faster than τ_{act}, presumably because a closing conformational change in just one subunit suffices to abolish conduction. Both H^+ and K^+ currents are inhibited by extracellular divalent cations like Zn^{2+} in most species by a mechanism in which τ_{act} is slowed drastically, the g-V relationship is shifted positively, and τ_{tail} is affected only weakly (36, 98, 101).

Proton currents in different species differ most obviously in gating kinetics. Mammalian proton currents activate with τ_{act} in the range of seconds at room temperature, whereas in snail neurons, τ_{act} is a few milliseconds. These kinetic differences are consistent with the proposed functions of proton channels in these cells. In most mammalian cells, proton currents extrude acid, which is not a job that needs to be rushed. Even when proton currents compensate charge in phagocytes (see Section "Charge compensation"), the kinetics of Nox activation is sufficiently slow that a rapid compensatory response is not necessary. However, in snail neurons, the proposed function is to open during action potentials (29, 167, 170, 242, 260), and consequently, speedy activation is essential.

Gating kinetics provides clues to and constraints on possible gating mechanisms. For example, as was discussed previously (see Section "Gene and molecular features") activation of proton current during depolarizing pulses is sigmoid in most species. As shown in Figure 4, this property reflects the dimeric nature of the channel, together with the apparent cooperativity in gating (103, 139, 198, 199, 261, 262). The greater complexity of channel opening in the dimer is reflected in the twice-stronger temperature dependence of both opening and closing kinetics in the dimer compared with the monomer (199). One intriguing feature of the temperature dependence of gating of native proton currents (Fig. 11) is that the Q_{10} (the factor by which a kinetic parameter changes with a 10°C change in temperature) was the same for all three parameters determined: delay, τ_{act}, and τ_{tail}; activation was fitted by a delay followed by a single rising exponential (67). All three parameters had Q_{10} 6-9, which is extraordinarily high for ion channel gating kinetics, which most frequently are near 3 (67, 119). The similarly high Q_{10} for all three gating parameters was interpreted to reflect a channel with multiple independent subunits, each of which must undergo a complex

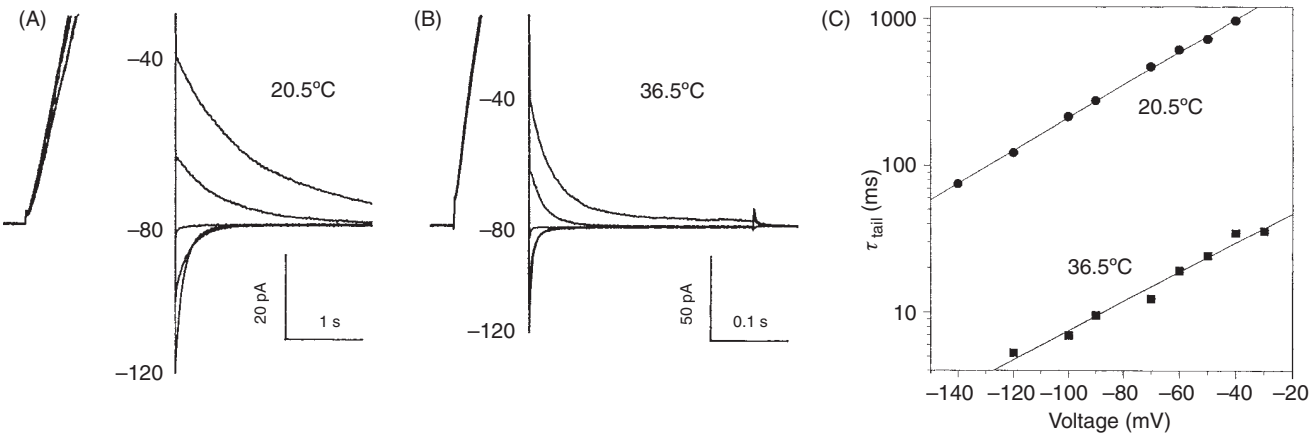

Figure 11 Proton channel gating is strongly temperature dependent. (A, B) In a human neutrophil at pH_o 7.0, pH_i 5.5 at the indicated temperatures, a depolarizing prepulse activated the g_H, then the voltage was stepped to test voltages, illustrated in 20-mV increments. Note the change in time base. The "tail current" (deactivation or closing) time constant, τ_{tail}, was obtained by fitting a single decaying exponential to each current. The Q_{10} was identical at all voltages (C) and was 8.5 in this cell, corresponding to an activation energy of approximately 38 kcal/mol. [Adapted, with permission, from reference (67) © DeCoursey & Cherny, 1998. Originally published in The Journal of General Physiology.]

gating transition during opening, with a reverse conformational change in only one subunit being sufficient to close the channel (67). This class of mechanism again resembles the classical Hodgkin-Huxley model for Na^+ and K^+ channel gating. The revelation that in many species, the proton channel functions as a dimer in which both protomers must undergo an opening conformational change before either can conduct (103, 199, 262) is in excellent agreement with the predictions that were based on temperature effects on gating kinetics.

Another clue to the gating mechanism comes from deuterium isotope effects. In most respects, proton channels functioned similarly in normal and heavy water. However, channel opening was 3-fold slower in deuterium, whereas channel closing was at most weakly affected (66). Because deuterons bind with higher affinity to most titratable groups, the slowing of activation by deuterium is consistent with deprotonation being a rate-determining step in channel opening. A 3-fold slowing is consistent with a 0.5 unit increase in the pK_a of the group in D_2O (66), which in turn is more consistent with a carboxylic or ammonium group being involved than a sulfhydryl acid (66, 238). Intriguingly, and perhaps coincidentally, both pH_o and D_2O have large effects on τ_{act} and small effects on τ_{tail}. Deprotonation of hypothetical groups accessible to the internal solutions was proposed to be a prerequisite step in channel opening in a model proposed to explain the dependence of the g_H-V relationship on both voltage and the pH gradient, ΔpH (38). In this model, the protonation state of titratable groups accessible to one side of the membrane or the other regulates proton channel gating (38).

Given their structural parallels (Fig. 2), it is tempting to assume that gating of H_V1 will entail the same outward movement of the S4 domain that is thought to occur in the VSD of K^+ and Na^+ channels (131, 147, 161, 253, 275, 276). Indeed, Cys scanning supports the general similarity of S4 movement in CiH_V1 to that of other VSDs (103), as do paddle motif swaps (7). However, a remarkable study of mH_V1 revealed that mutants in which the entire C terminus was truncated along with S4 as far as between the second and third Arg residues in the S4 domain still retained proton channel function (230). Although each of the three S4 Arg residues in H_V1 contributes to voltage sensing (104), their movement must not be as extensive as in K^+ channels, unless the movement in the C truncated mutant was reduced compared to the WT channel. The charged residues in S4 of the Shaker K^+ channel VSD are proposed to move through a "gating charge transfer center" (258); the first (R1) is in this center in closed channels, but the fifth (K5) resides there in the open state (157).

At present, most fundamental questions regarding gating remain unanswered or incompletely answered. What is the structural difference between open and closed proton channels? How does the molecule move during gating? How do the two protomers interact during gating in the dimer? How does pH regulate the voltage-dependence of gating? Although recent discoveries resulting from structure-function studies seem to have complicated rather than clarified these questions, the voltage-gated proton channel continues to be an exceptional system in which to explore fundamental questions about voltage gating mechanisms.

Inhibition of proton currents by Zn^{2+} is surprisingly revealing

Essentially every study that has reported the existence of proton currents in a new cell type has used inhibition by Zn^{2+} as a defining feature. Occasionally, Cd^{2+} or other polyvalent metals are included; a large number have generally similar effects, including Cu^{2+}, Ni^{2+}, Co^{2+}, Mn^{2+}, Be^{2+}, Pb^{2+}, Hg^{2+}, La^{3+}, Gd^{3+}, and Al^{3+}, with Zn^{2+}, Cu^{2+}, and La^{3+} considered the most potent (56). In fact, in the absence of other high-affinity inhibitors, Zn^{2+} is frequently used to antagonize

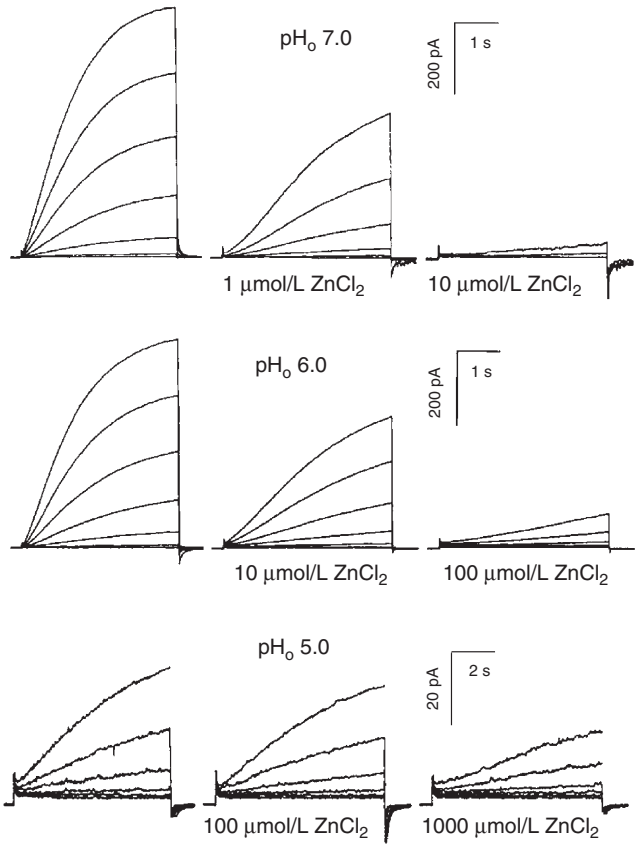

Figure 12 Modulation of Zn^{2+} effects on proton currents by pH_o reveals strong competition between Zn^{2+} and H^+ for external binding sites. Identical families of pulses were applied in each row at the indicated pH_o and Zn^{2+} concentrations. Zn^{2+} slows activation of the proton current at a given voltage and shifts the g_H-V relationship positively. [Adapted, with permission, from reference (36) © Cherny & DeCoursey, 1999. Originally published in The Journal of General Physiology.]

physiological effects of proton channel function in cells. The advent of the *HVCN1* knockout mouse has provided an alternative to this classical pharmacological lesion experiment. As more homologs of proton channels are identified and characterized, some have been discovered to be relatively insensitive to inhibition by Zn^{2+}. The proton channel of the sea squirt, *C. intestinalis*, can be inhibited by Zn^{2+}, but only at concentrations 27-fold higher than the mouse channel (234). A proton channel in *E. huxleyi*, a marine phytoplankton, is also only weakly inhibited by Zn^{2+} (259), as is kH_V1, a dinoflagellate channel (unpublished data with S.M.E. Smith, D. Morgan, B. Musset, V.V. Cherny, A.R. Place, and J.W. Hastings). Thus, there is a hint of a pattern of weaker metal sensitivity for proton channels in marine than terrestrial life. However, proton currents in the nudibranch mollusc, *Tritonia diomedea*, appear to exhibit high Zn^{2+} sensitivity (271), as do proton currents in *C. pelagicus*, a marine coccolithophore (259). In any case, the idea that lower Zn^{2+} sensitivity in marine species might be a protective adaptation to the heavy metal content of seawater seems unlikely, because the metal concentrations are too low to produce much inhibition of even the more sensitive human proton channel: 76 nmol/L Zn^{2+}, 112 nmol/L Ni^{2+}, 14 nmol/L Cu^{2+}, 1 nmol/L Cd^{2+}, and 21 pmol/L La^{3+} (263). Low sensitivity to metal will become more important as the seas become polluted, but at present there seems to be a reasonable safety factor.

The effects of polyvalent cations on voltage-gated proton channels resemble the effects of these metals on most voltage-gated ion channels. Metal ions slow channel opening, shift the g-V relationship positively, and may reduce the maximum conductance (36, 89, 119). As illustrated in Figure 12, although Zn^{2+} appears to make the current smaller, most of this is the result of slower activation kinetics (larger τ_{act}) and a positive shift of the g_H-V relationship. Both of these effects were quantified over a range of pH_o and the pattern was evaluated using several possible models of competition. Ironically, despite the widespread use of Zn^{2+} to characterize proton currents, one of the most remarkable features of the inhibition of proton currents by Zn^{2+}, namely, the strong modulation of Zn^{2+} effects by pH, was overlooked until 17 years after the first report of voltage-gated proton channels (36). To a first approximation, the inhibition produced by 1 µmol/L Zn^{2+} at pH_o 7.0 requires 10 µmol/L Zn^{2+} at pH_o 6.0, and approximately 1000 µmol/L Zn^{2+} at pH_o 5.0 (Fig. 12). The antagonism between low pH and Zn^{2+} suggests that H^+ and Zn^{2+} complete for a binding site on the proton channel molecule.

Figure 13 illustrates the predictions of the preferred model in which Zn^{2+} binds competitively with H^+ at three sites with pK_a 6.3, a metal-binding constant pK_M 6.5, and a

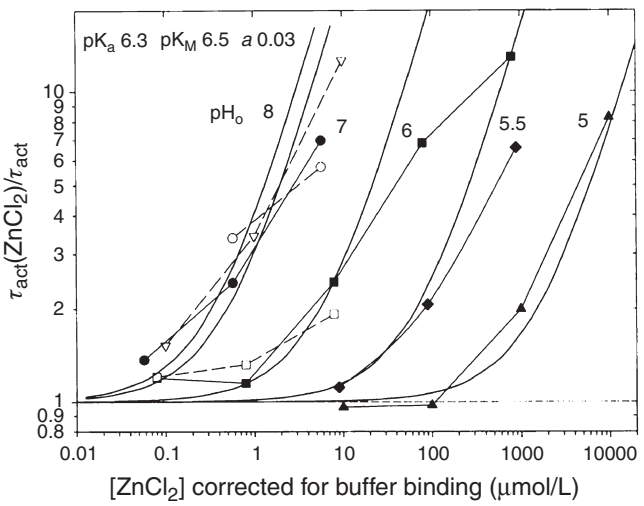

Figure 13 The pH_o dependence of the slowing of proton current activation can be explained if Zn^{2+} binds to a site consisting of three groups with pK_a 6.3, with affinity 316 nmol/L, and cooperativity factor $a = 0.03$ (see text). All curves were drawn with these values and no other adjustable parameters. Adequate fits were also obtained by assuming two titratable groups, but not with only one. At high pH_o competition with protons disappears and limits to simple metal binding. See text for further details. [Adapted, with permission, from reference (36) © Cherny & DeCoursey, 1999. Originally published in The Journal of General Physiology.]

cooperativity factor of 0.03, meaning that Zn^{2+} can still bind if one of the three groups is protonated, but with approximately 30-fold lower affinity. There were no other adjustable parameters in the model, which simply assumed that the proton channel cannot open when Zn^{2+} is bound (36). Two other, even simpler models also provided good fits to the data; these had two or three titratable groups that coordinated Zn^{2+} strictly competitively with protons. In contrast, simple 1:1 competition could not explain the data, because the effectiveness of Zn^{2+} decreases by a maximum of 10-fold/unit pH in such a model, and the data clearly indicated a 100-fold shift between pH_o 6 and pH_o 5 (Figures 12 and 13). The outcome of this exercise was a prediction that Zn^{2+} inhibits proton currents by binding simultaneously to at least two groups with pK_a 6-7, in the range of His (36). This prediction appeared to be borne out nicely when the human proton channel was identified 7 years later. Ramsey and colleagues (224) showed that two His residues, His^{140} and His^{193}, that were expected to be accessible to the external solution, both contributed to Zn^{2+} inhibition.

To our consternation, a homology model of the human proton channel structure, based on the crystal structure of the VSD from K^+ channels, indicated that the two Zn^{2+}-binding His residues, His^{140} and His^{193}, were approximately 14 Å apart, too far to plausibly coordinate a single Zn^{2+} atom (199). Another homology model predicted a comparable separation between the two His residues (223). However, the discovery that the proton channel was a dimer (139,150,261), presented a possible explanation. As shown in Figure 5B, if the dimer adopts a position with the complementary His residues facing each other, Zn^{2+} could bind at the interface between the protomers. This hypothesis was explored by creation of a series of channels with mutations to His^{140} and His^{193} as well as tandem dimers. Figure 14A and B illustrates the generally similar pattern observed for Zn^{2+} shifting the g_H-V relationship and slowing activation, respectively. Mutation of either His^{140} (H140A) or His^{193} (H193A) individually attenuated Zn^{2+} effects, indicating that both residues contribute to the effects observed in WT channels. H140A, H193A and the tandem dimer H193A-H140A all exhibited distinct Zn^{2+} effects that were weaker than in WT. Remarkably, the tandem dimer WT-H140A/H193A was as insensitive to Zn^{2+} as the double mutant that lacked both His (H140A/H193A). In particular, the slowing effect of Zn^{2+} occurs only when there is at least one His in each protomer, and is absent when both His are present in the same protomer. This pattern suggests that Zn^{2+} slows proton channel opening when it binds at the interface between protomers. Presumably, the Zn^{2+}-bound channel dimer cannot undergo a conformational change required for opening.

Functions

As discussed previously (see Section "Regulation of gating by the pH gradient, ΔpH"), the properties of the voltage-gated proton channel suggest that in most species, this molecule is ideally suited to solve "the central problem of pH_i regulation: the neutralization of intracellular acid derived from a variety of sources" (228). Proton channels have been shown to contribute to pH_i recovery following an acid load in a variety of cells: snail neurons (260), rabbit osteoclasts (211), human neutrophils (75), mouse mast cells (145), rat microglia (187), a human bronchial epithelial cell line (16HBE14o-) (264), rat alveolar epithelial cells (192), rat hippocampal neurons (35,246), murine osteoclasts (183), TsA201 cells transfected with the mouse proton channel gene *mVSOP* (234), and in a rat microglial cell line GMI-R1 (185). In many other cells, proton channels extrude acid under specific conditions that occur physiologically. Hypotonic shock leads to depolarization and alkalinization in bovine articular chondrocytes that may be mediated by proton channels (231, 232). Roles in regulating both pH_i and membrane potential have been proposed in human cardiac fibroblasts (87). Although acid extrusion remains the main general function of proton channels, several quite different functions have been identified in a number of cells, which are described in the following Sections.

Bioluminescence and other functions in dinoflagellates

As mentioned previously (Fig. 1), the first explicit proposal of a voltage-gated proton channel was in 1972 by Fogel and Hastings in the bioluminescent dinoflagellate, *G. polyedra* (96). It had been shown previously that current injection into the large central vacuole of another bioluminescent dinoflagellate, *Noctiluca scintillans (N. miliaris)*, elicited an all-or-nothing action potential that appeared to be inverted (34, 120). Elegant studies by Roger Eckert and colleagues showed that the *Noctiluca* action potential occurs across the tonoplast, the membrane surrounding the large central flotation vacuole, and is inverted when recorded by a pipette inserted into the vacuole, because this is the topological equivalent of extracellular recording (80,81,83). The action potential triggers luminescence that originates in numerous discrete sources (80,81,82,83, 220). These microsources have been named "scintillons" (78, 111), and are filled with luciferin, luciferase, and luciferin binding protein (95, 96, 237). Figure 15 illustrates the mechanism by which proton channels are thought to participate in dinoflagellate bioluminescence. Upon mechanical stimulation (e.g., by a breaking wave, the wake of a passing boat, or the splashing of a nocturnal swimmer), an action potential travels along the tonoplast (81) and invades the scintillon. Scintillons are connected by a neck of membrane that is continuous with the tonoplast (209). The action potential depolarizes the scintillon membrane, opening proton channels, which mediate proton flux from vacuole into the scintillon. The vacuole has very low pH, estimated to be 3.5 in *Noctiluca* (205), whereas the scintillon is near neutral, so there is a large chemical driving force. The protons trigger a light flash by changing the activities of two proteins. First, luciferin-binding protein releases luciferin, the light-emitting substrate of luciferase, at low pH

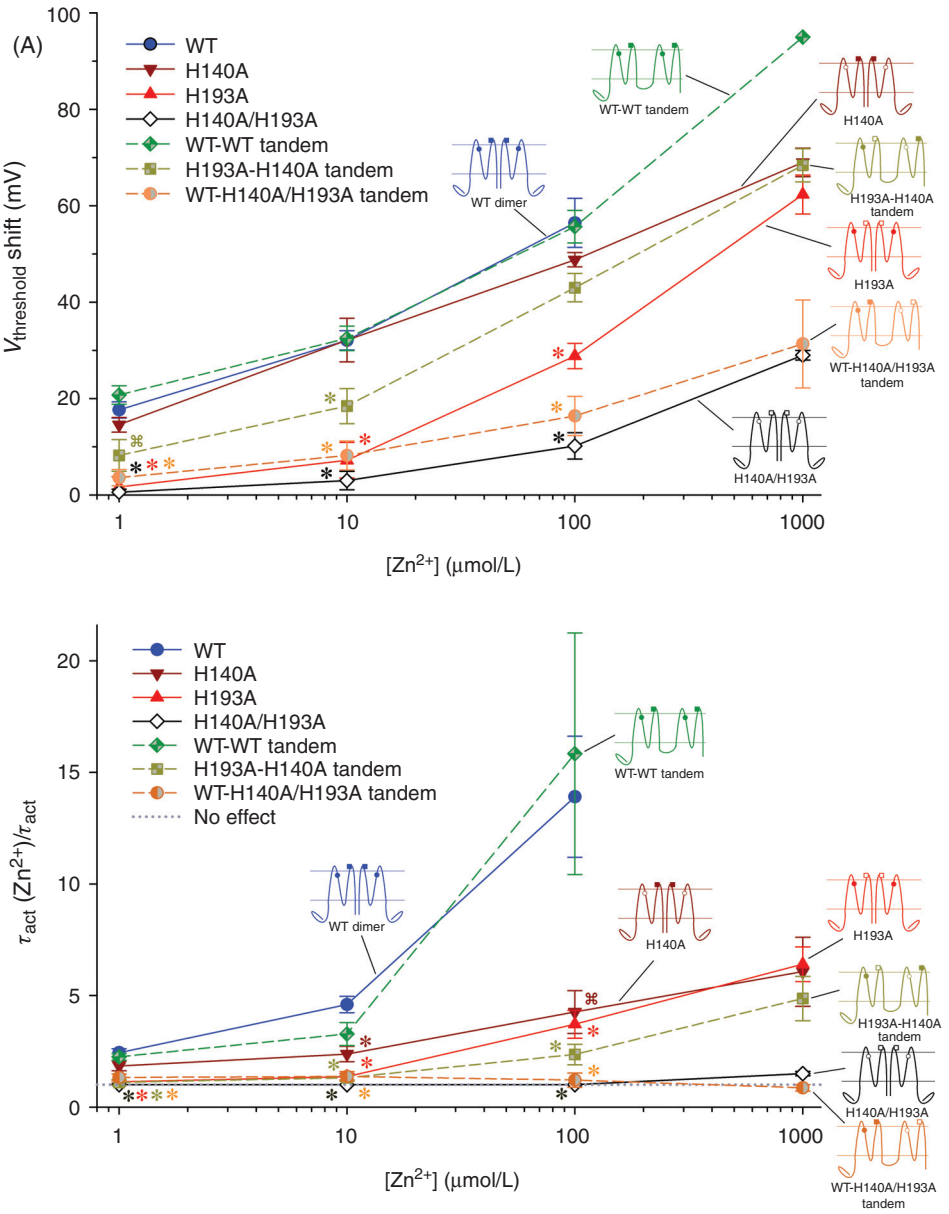

Figure 14 Effects of Zn^{2+} on $V_{threshold}$ (A) and on the slowing of proton current activation (B) in constructs with several His mutations. Dimeric proton channels are illustrated with diagrams in which solid symbols indicate His and open symbols indicate Ala substituted for His. Three tandem dimers are shown with their C- and N-termini linked to constrain the His positions in the dimer. $V_{threshold}$ shifts were estimated from g_H-V relationships plotted semilogarithmically. Statistical comparisons are to WT channel parameters (⌘$P < 0.05$, *$P < 0.01$). [Adapted, with permission, from reference (199). Originally published in The Journal of Physiology 588:1435-1449, 2010.]

(25,95,141). Second, luciferase has a pH optimum at pH 6.3, and is inactive at pH 7.5 (141,237). It seems very likely that voltage-gated proton channels play a crucial role in triggering bioluminescence in dinoflagellates, by orchestrating the concerted activation of both mechanisms.

A further, more spectacular role has been speculated to exist, namely, mediating the action potential itself (209). The flash-triggering action potential coincides with decreased impedance, indicating that a conductance increase is responsible (83). The peak of the action potential is not affected by various ion substitutions in the vacuole (205), but when pH in the vacuole was increased, the peak decreased (206) as expected if proton flux mediates the action potential. A voltage-gated proton channel gene from a nonbioluminescent dinoflagellate, *K. veneficum* (22) has been identified and expressed heterologously (250). *K. veneficum* is a predatory dinoflagellate notorious for producing a variety of toxins (247); its blooms coincide with fish kills in coastal waters worldwide (13,74). Remarkably, although the expressed kH_V1 protein exhibits all of the main features of voltage gated proton

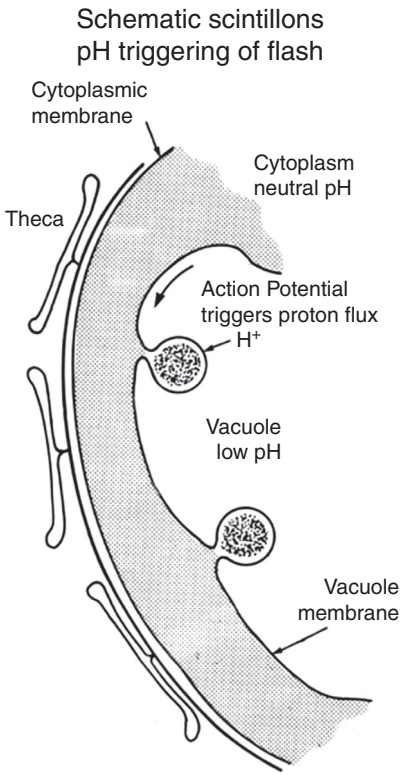

Figure 15 Proposed mechanism by which proton flux through voltage-gated proton channels triggers light flashes in dinoflagellates. Mechanical stimulation elicits an action potential conducted along the tonoplast, the membrane separating the central vacuole and a thin layer of cytoplasm (gray). When the action potential invades the scintillons (grape-like structures formed by evagination of tonoplast), proton flux from the vacuole at low pH into the scintillon activates luciferase, triggering the flash. [Adapted, with permission, from reference (110). Originally published in Hastings JW. Bioluminescence. In: *Cell Physiology Sourcebook: A Molecular Approach* (3rd ed.), Sperelakis N, editor. San Diego: Academic Press, 2001, p. 1115-1131.]

channels in other species, including obeying the Rule of Forty [Eq. (4)], it differs in the absolute position of the g_H-V relationship. As illustrated in Figure 10, at any given ΔpH, the kH_V1 channel opens at voltages 60 mV more negative than in all other species (251). Consequently, there is a substantial voltage range within which inward H^+ current occurs. These properties are reminiscent of voltage-gated Na^+ channels and strongly suggest the ability of these channels to mediate an action potential. In any case, the negative voltage range of activation of kH_V1 indicates a stark difference in function, compared with all other known proton channels. Whereas other proton channels are designed to allow only proton extrusion; kH_V1 activation will produce H^+ influx. H^+ influx could initiate or propagate action potentials, or produce a drop in pH_i that might have signaling functions. A role of H^+ flux into the cytoplasm was proposed to trigger tentacle flexion in *N. miliaris* (212). As originally proposed (96), H_V1-mediated H^+ flux from the vacuole into the scintillon triggers the flash (251) (Fig. 15).

A variety of functions might exist for proton channels in nonbioluminescent dinoflagellate species. For example, in mixotrophic species like *K. veneficum*, H^+ flux might be involved in capturing prey by extrusion of trichocysts or prey digestion. A phylogenetic analysis of VSD regions from several dozen H_V1 sequences revealed high sequence diversity among the single-celled species and among invertebrates (Fig. 3). Although this observation may partially reflect the genetic liability of dinoflagellates and other unicellular species (11), diverse sequences could well produce other novel functions of H_V1. As in multicellular organisms, ion channels in dinoflagellates undoubtedly play a variety of roles in regulating basic life functions, which makes them excellent targets for controlling dinoflagellate populations and behavior.

Calcification by coccolithophores

New proton channel genes were recently identified in two marine unicellular algae, the coccolithophores *E. huxleyi* and *C. pelagicus ssp braarudii* (259). The properties of these channels in heterologous expression systems were quite similar to those of other species, with the exception that the *E. huxleyi* channel (EhH_V1) was only weakly inhibited by Zn^{2+}. Coccolithophores are abundant phytoplankton that play a major role in calcification; that is, the conversion of HCO_3^- (derived from CO_2 dissolved in ocean water) into calcium carbonate, $CaCO_3$ via the intermediate reaction $HCO_3^- \rightarrow CO_3^{2-} + H^+$. Each Ca^{2+} that is converted into $CaCO_3$ generates a proton, which must be eliminated from the cytosol of the coccolithophore. Inhibiting the Zn^{2+}-sensitive CpH_V1 with 30 μmol/L Zn^{2+} produced an immediate drop in pH_i and a sustained decrease in calcite production (259). Decreasing pH_o lowers pH_i, suggesting that ocean acidification due to dissolution of atmospheric CO_2 derived from human activity (or, for those who harbor doubts as to its source, by magic) could inhibit calcification directly. However, a stronger correlation was found between coccolith mass and $[CO_3^{2-}]$ than with pH or pCO_2, indicating complex control (21). Nevertheless, since the Last Glacial Maximum (ice age), ocean CO_2 levels have increased by approximately 50% (from ~190 to ~280 parts per million), and coccolith mass has decreased by almost 50% (from 13.6 to 7.5 pg) (21).

Acid extrusion during action potentials in snail neurons

The first voltage-clamp studies of proton channels were in garden snail neurons, *H. aspersa* (260). Similar proton currents exist in the pond snail, *L. stagnalis* (29). The most unusual feature of proton currents in snail neurons is their rapid gating kinetics (Fig. 16), with both activation and deactivation occurring in a few tens of milliseconds or less (29, 167). The rapid activation kinetics is consistent with the proposal that proton channels open during action potentials, and extrude acid to counteract the rapid intracellular acidification that occurs in these neurons during trains

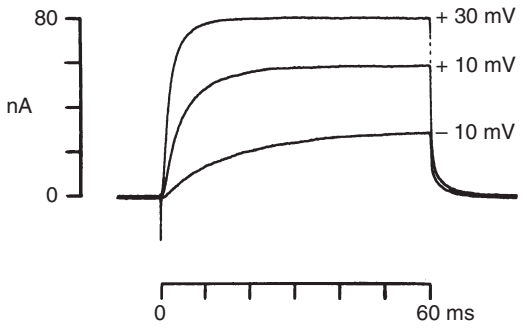

Figure 16 Rapidly activating proton currents in a *Lymnaea* snail neuron, 120 μm in diameter. Currents during pulses to the voltages shown at pH_o 7.4, pH_i 5.9 at room temperature. [Adapted, with permission, from reference (29). Originally published in The Journal of Physiology 351:199-216, 1984.]

of action potentials (5, 29, 167, 260). Activation of proton channels in *H. aspersa* axons by depolarization generates alkalinization that is nonuniform due to geometrical factors, resulting in pH_i microdomains (214, 242).

A similar role of opening to extrude acid during action potentials was suggested for proton channels in human skeletal muscle myotubes (24).

Amphibian oocytes and fertilization

Voltage-gated proton currents in *Ambystoma* oocytes have slower kinetics than those in snail neurons, but faster than in most mammalian cells, with τ_{act} of a few hundreds of milliseconds (19). The idea that proton channels might contribute to the alkalinization of oocytes during fertilization (19) is supported by a gradual decrease in proton current density within hours after fertilization (20). *Xenopus laevis* oocytes alkalinize by an average of 0.18 pH unit during progesterone-induced maturation; and exogenously induced alkalinization triggers maturation; however, the correlation is not absolute (149).

Frog (*Rana esculenta*) oocytes have slowly activating proton currents that were suggested to play a role during fertilization similar to that in *Ambystoma* (126). A more specific role of promoting inositol triphosphate ($InsP_3$) receptor-mediated intracellular Ca^{2+} oscillations was later elaborated (125).

The zinc theory of fertilization by human sperm

Human sperm are blessed with abundant proton channels, with a proposed role somewhat like that postulated in oocytes, namely, the production of an intracellular alkalinization during events associated with fertilization. Sperm from humans and other animals undergo several changes in their motility as they undergo "capacitation," the maturation process that occurs after sperm enter the female reproductive tract and that is prerequisite to fertilization. Some of those changes are mediated by increased pH_i, which stimulates metabolic activity and motility of sperm (9). Studied *in vitro*, the alkalinization is sensitive to membrane potential and in some species appeared to reflect an increase in membrane proton permeability (8). However, indirect monitoring of the activity of voltage-gated proton channels by pH measurements did not provide definitive demonstration of their presence in sperm (8, 9). The discovery of a way to patch-clamp sperm finally confirmed that voltage-gated proton channels are present in human sperm (160). Proton currents were larger in capacitated sperm, and capacitation *in vitro* was inhibited by Zn^{2+} (160), leading to a "zinc hypothesis" that proposes that Zn^{2+} is necessarily removed from sperm during the course of capacitation. Seminal fluid has a high concentration of zinc at 2.2 mmol/L (229), but this value reflects total concentration, not free Zn^{2+}. [For instance, equine plasma contains 8 μmol/L total zinc, but only 210 pmol/L free Zn^{2+} (165)]. Assuming that sufficient Zn^{2+} is present to inhibit proton channels, pH_i would remain low until the sperm approach their destination inside the female reproductive tract where they encounter a more hospitable environment replete with proteins to buffer Zn^{2+}. Thus relieved of their inhibitions, proton channels would conduct H^+ out of the cytoplasm, pH_i would increase, and the sperm would capacitate and forge ahead to fertilize the ovum. This remarkable hypothesis may apply to humans, but cannot explain sperm alkalinization in mouse, whose sperm apparently lack proton channels (160). No fertility defects have been reported in *HVCN1* knockout mice. In the Japanese eel, *Anguilla japonica*, spermatogenesis as well as sperm motility *require* Zn^{2+} (274).

Acid secretion in epithelia of the respiratory tract

Voltage-gated proton currents are present throughout the epithelium of the respiratory system, from alveolar epithelium (54) to tracheal epithelium (94) to nasal and sinus mucosa (44). Both the alveolar lining fluid and airway surface liquid are maintained at relatively low pH (93, 210). The primary mechanism of H^+ secretion by airway epithelial cells—both human airway cell lines and primary cultured airway tissues—is the voltage-gated proton channel, with smaller contributions from other transporters (44, 94, 128, 240). Proton secretion measured in chronic rhinosinusitis patients increases in asthma, and the fraction contributed by proton channels decreases (44).

Acid secretion in airway epithelia was inhibited equally by Zn^{2+} or by Nox inhibitors, suggesting that oxidase activity generates a proton gradient that drives H^+ secretion via proton channels (240). The main Nox system in human fetal lung epithelial cells is DUOX1 (92); DUOX is also present in adult human airway epithelium (97). DUOX activity may serve a host defense mechanism in airway cells akin to that in phagocytes (97, 208, 240). In airway epithelial cells, ATP-stimulated H_2O_2 production corresponding to approximately 3 to 340 fA (97, 188) and in alveolar cells hormone-stimulated H_2O_2 production of approximately 21 fA of electron current per cell were found (92). The disparate values for H_2O_2 production in cultured airway cells may reflect a strong dependence

of DUOX expression on time in culture (221). Because these cells have abundant other conductances, it is not clear whether proton channels are necessary to compensate such a small electrogenic flux (91).

It was hypothesized that proton channel-mediated H^+ efflux in alveolar epithelial cells might contribute to CO_2 elimination by the lung (55), although this would occur slowly due to the absence of carbonic anhydrase in apical subphase liquid (84). Several attempts to evaluate this mechanism have failed to support the idea (85,133,255), but conclusive studies have not been reported.

The first proton channel mutation to be identified in a human subject was Met^{91} to Thr (M91T) (128). The source of the M91T mutation was deceased and had an unremarkable clinical history. Only one heterozygous M91T genotype was detected in 95 human genomic DNA samples, placing an upper limit on its frequency of occurrence. Channels with the M91T mutation in heterologous expression systems were activated in a more positive voltage range than normal (WT) proton channels. Because airway epithelial cells are thought to maintain a relatively constant membrane potential, under physiological conditions proton channels are most likely activated by an increased outward pH gradient (cytoplasmic acidification or mucosal alkalinity or both) (128). The M91T mutant would require a pH gradient approximately 0.5 unit larger to activate the g_H to the same extent (128).

B-cell receptor signaling in human B-lymphocytes

Voltage-gated proton channels are expressed in every leukocyte or related cell line that has been studied, but expression levels vary greatly. Human T-lymphocytes have barely detectable proton currents, averaging 1.5 pA at +60 mV in whole-cell recordings at pH_o 7.5 and pH_i 6.0, but proton currents in human B-lymphocytes are more than 100 times larger (236). Staining with an hH_V1 antibody reveals high levels of protein expression in peripheral B cells, but undetectable levels in T cells (32). The expression of hH_V1 protein in human tonsillar tissue was high in resting cells, but downregulated in proliferating cells in the germinal centers, suggesting a role in early stages of B cell activation (32). The proton channel protein colocalized with the B cell receptor (BCR) during capping and receptor internalization and was coimmunoprecipitated with the BCR-associated protein Igβ, indicating physical proximity of the two molecules (32).

Unlike the bactericidal role of reactive oxygen species (ROS) produced by phagocytes (see Section "The phagocyte respiratory burst"), B cells produce ROS mainly for

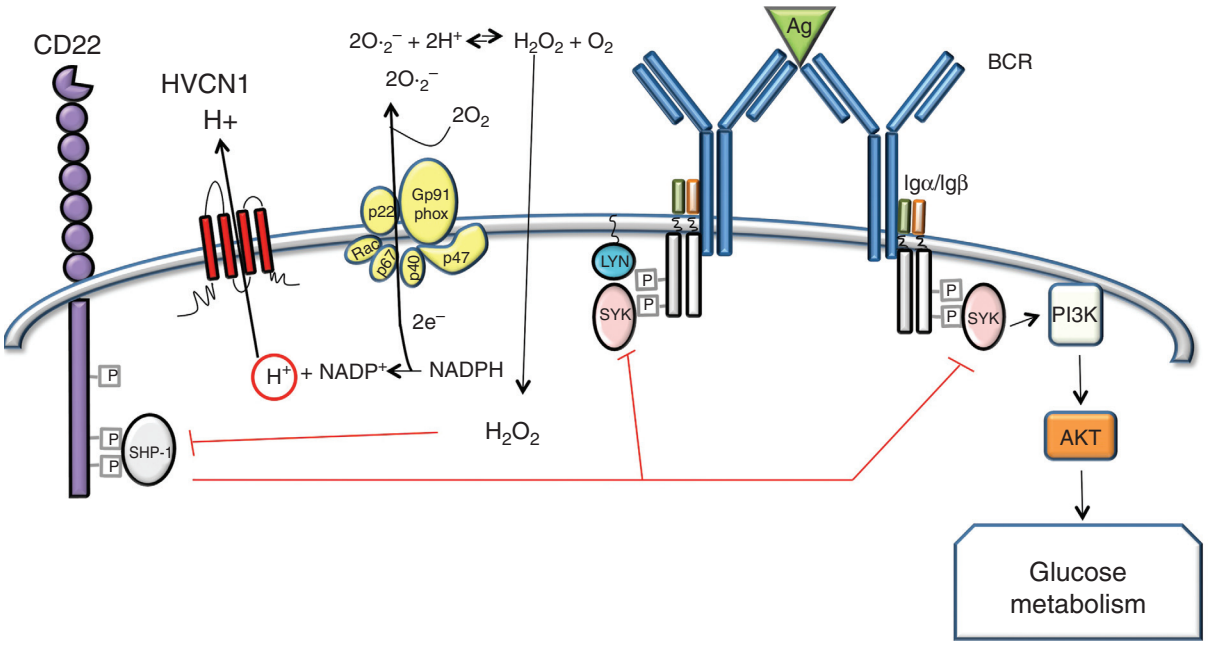

Figure 17 Schematic representation of the role of the proton channel (HVCN1) in the context of B cell receptor (BCR) stimulation. Antigen binding to the BCR results in phosphorylation of immunoreceptor tyrosine activation motif (ITAMs) in the Ig-α/β heterodimer by LYN, creating docking sites for Syk. This serves to amplify BCR signaling by further recruitment and activation of Syk, which leads to PI3K activation, activation of Akt and increased glucose uptake and metabolism. Amplification of signaling is negatively regulated by CD22, which is also phosphorylated by LYN, providing a docking site for protein tyrosine phosphatase SHP-1. In resting cells, SHP-1 inhibits B cell activation by dephosphorylating Syk, thus counterbalancing ITAM-Syk mediated signal amplification. BCR stimulation results in reactive oxygen species (ROS) generated by NADPH oxidase. The $O_2\cdot^-$ that is produced combines with protons to form H_2O_2 and O_2, which freely diffuse through the membrane. ROS generate a localized oxidizing environment causing inhibition of SHP-1, which results in amplification of BCR signal. HVCN1 sustains NADPH oxidase activity. In the absence of HVCN1, the oxidizing environment cannot be maintained and consequently SHP-1 remains active, reducing BCR-signal strength. [Adapted, with permission, from reference (32). Originally published in *Nature Immunology* 11: 265-272, 2010.]

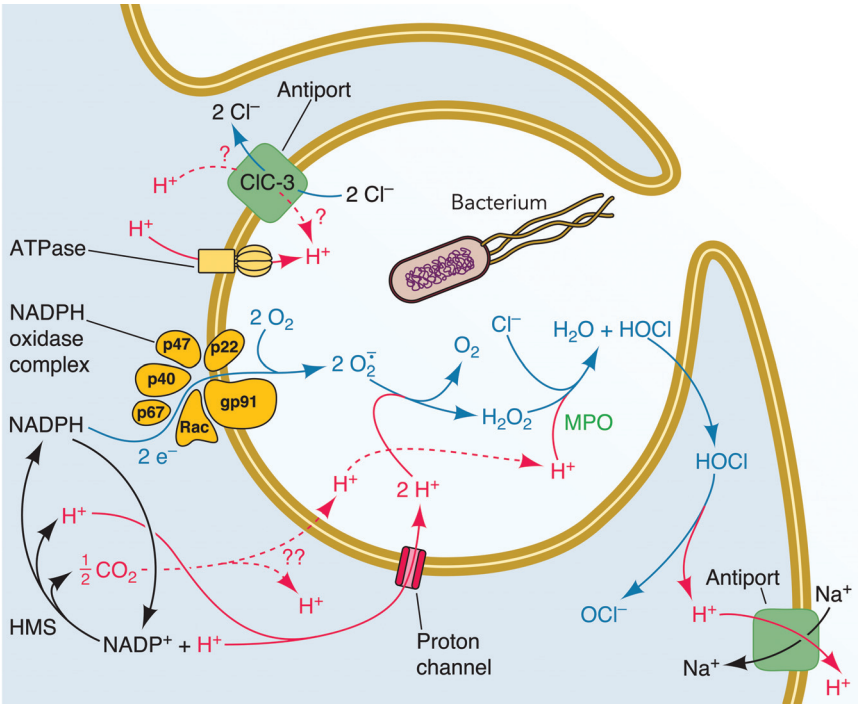

Figure 18 Proton husbandry during the phagocyte respiratory burst. Upon stimulation, the components of the NADPH oxidase complex assemble at the membrane and begin to relay electrons from NADPH across the membrane to reduce O_2 to superoxide anion, $O_2^{\cdot -}$. Because of the massive increase in O_2 consumption, this process is called the "respiratory burst" (12) despite the fact that most of the O_2 is consumed to make reactive oxygen species (ROS) and it is not affected by mitochondrial inhibitors (235). Protons left behind in the cytoplasm exit mainly through voltage-gated proton channels (193), although other transporters also play important roles (178). Inside the phagosome, protons are consumed during the spontaneous dismutation of $O_2^{\cdot -}$ to H_2O_2 as well as during HOCl generation by myeloperoxidase (MPO) (138). [Adapted, with permission, from reference (58). Originally published in *Physiology* 25: 27-40, 2010.]

signaling. The somewhat daunting pathways involved are summarized in Figure 17. ROS production by splenic B cells stimulated by either PMA or anti-IgM was greatly reduced in the *HVCN1* knockout mouse (32). ROS are required to inhibit phosphatases temporarily and thus allow correct B cell activation. Most of the deficits in B cell function in the *HVCN1* knockout mouse could be explained as consequences of perturbed downstream signaling due to impaired oxidation of the protein tyrosine phosphatase SHP-1 (32, 227).

The phagocyte respiratory burst

Charge compensation

The best-known specific function of voltage-gated proton channels is charge compensation in phagocytes. This role is quite distinct from acid extrusion, although the latter inevitably occurs at the same time. Henderson, Chappell, and Jones pioneered this area of study in the late 1980s, publishing a series of groundbreaking papers (115, 116) that drew three crucial conclusions. First, they showed that Nox, the enzyme activated in neutrophils, macrophages, and eosinophils during phagocytosis (Fig. 18), is electrogenic. The electron transfer pathway is located in the $gp91^{phox}$ component of Nox, which has been renamed Nox2 (sometimes the entire Nox complex is imprecisely called Nox2). Electrons are transferred from intracellular NADPH across a redox chain comprising FAD (flavin adenine dinucleotide) and two heme groups to extracellular (or intraphagosomal) O_2 to form superoxide anion ($O_2^{\cdot -}$) (10). The flux of electrons across the membrane has two immediate consequences: depolarization and pH changes. The membrane potential will depolarize rapidly; without compensation, the electron current in a human eosinophil at 37°C would depolarize the membrane at a rate greater than 18 volt/s (56). It is obvious that charge compensation is necessary to prevent membrane dielectric breakdown. Somewhat less obviously, depolarization itself inhibits Nox activity, especially positive to +50 mV (73), which happens to be roughly the level of depolarization attained by intact human neutrophils at the peak of the respiratory burst (100, 130, 222). Depolarization to +200 mV abolishes Nox activity altogether (73, 216). The depolarization of the plasma membrane during Nox activity is exacerbated by Zn^{2+} (or Cd^{2+}) at concentrations that inhibit proton currents, supporting the idea that proton channels contribute significantly by limiting the extent of depolarization (16, 17, 77, 88, 114, 146, 193, 222). Similarly,

the phagosome membrane depolarizes rapidly after phagosome formation (182). Limiting the extent of depolarization is also important for Ca^{2+} signaling, because it influences the driving force for Ca^{2+} influx through store-operated Ca^{2+} channels. The rise in intracellular Ca^{2+} elicited by chemoattractants was greatly attenuated in *HVCN1* knockout mice, but could be restored by collapsing the membrane potential with gramicidin (88).

Regulation of pH

The second major consequence of Nox activity is to change pH on both sides of the membrane, decreasing pH_i and increasing pH_o. For each electron that leaves the cytoplasm, one proton is left behind, either during the reduction of FAD or during the reconstitution of NADPH by the hexose monophosphate shunt (HMS in Fig. 18) (129). The HMS must operate continuously during the respiratory burst. To sustain an electron current of −10 pA, it was estimated that the entire cytoplasmic NADPH supply (50-100 μmol/L) must turn over 4 to 8 times/s (180); the respiratory burst lasts minutes to hours depending on the cell type and stimulus (72). The complex events depicted in Figure 18 can be best understood by realizing that Nox is the driving force for nearly everything else. Although at the peak of the respiratory burst, proton and electron fluxes are nearly identical (26, 257, 265), Nox gets off to a faster start than proton channels do. The most rapid consequence of oxidase activity is membrane depolarization. Because relatively few electrons must cross the membrane to change the membrane potential, compared with the amount of ROS that must be produced for biochemical detection, many early studies concluded incorrectly that membrane depolarization preceded and perhaps triggered the respiratory burst (31, 45, 132, 140, 243, 249, 268). The main charge compensators, voltage-gated proton channels, do not open until there has been sufficient depolarization, and thus will inevitably lag behind. Figure 19A illustrates that a rapid spike of acidification occurs simultaneously with phagocytosis in human neutrophils (178). In most cells, this was followed by rapid recovery. Pharmacological inhibition of several candidates indicated that the Na^+/H^+ antiporter and voltage-gated proton channels were both required for recovery. When H-ATPase was inhibited, only a small additional acidification of 0.14 units occurred, which became evident approximately 10 min after the initial phagocytotic event, indicating that the proton pump plays at best a minor role. Inhibiting Na^+/H^+ antiport or proton channels resulted in profound monotonic acidification to pH_i 6.14 or 5.87, respectively, after 14 min, levels that would strongly inhibit Nox (180). As may be seen in the example in Figure 19D, among the inhibitors tested, only Zn^{2+} affected the initial rate of acidification, doubling it (178). This indicates that the voltage-gated proton channel is the first H^+ transporter to respond during phagocytosis.

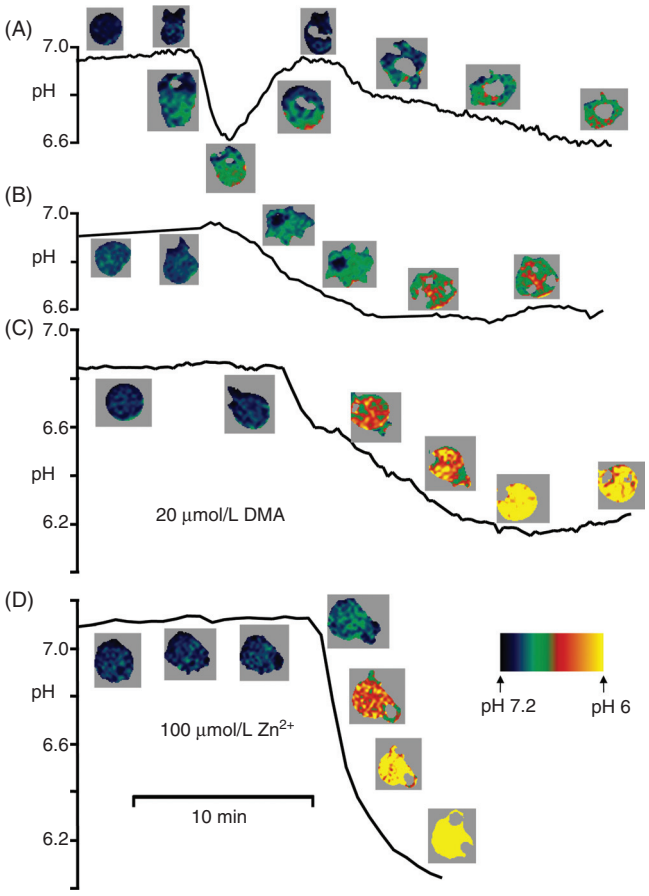

Figure 19 The pH_i in four individual human neutrophils during phagocytosis of opsonized zymosan (OPZ) is plotted, with pseudocolor confocal images of each cell at corresponding times. The cells were loaded with the pH sensing dye, SNARF-1. In control cells, pH_i drops rapidly when OPZ is ingested and often recovers rapidly (A), but in some cells does not (B). Recovery is prevented by 20 μmol/L dimethylamiloride, which inhibits the Na^+/H^+ antiporter (C) or 100 μmol/L Zn^{2+}, which inhibits proton channels (D). Among the inhibitors tested, only Zn^{2+} increased the rate of acidification, indicating that proton channels contribute significantly at early times. [Adapted, with permission, from reference (178). Originally published in Proceedings of the National Academy of Sciences, USA 106: 18022-18027, 2009.]

Other roles in phagocytes

In summary, there is clear evidence that proton channels contribute to both charge compensation and pH_i regulation during the phagocyte respiratory burst. Proton currents play at least two additional roles. Protons conducted into phagosomes act as substrate for the production of H_2O_2 and HOCl, the predominant early products of Nox activity (Fig. 18) (107, 193). The choice of protons, rather than other ions, as the main charge-compensating ion is sensible when one considers the magnitude of the task. Within a few minutes, the electrons entering through Nox would reach a virtual concentration of up to 4 mol/L inside the phagosome (107, 226), if they were not immediately consumed in ROS production. If these electrons were compensated by any cation besides H^+, the osmotic effect would be an approximately 20-fold swelling

of the phagosome, which does not occur. However, when H^+ compensates the electron flux, the protons and electrons end up mainly in the form of H_2O, HOCl, or H_2O_2, all of which are membrane permeant, thus minimizing osmotic swelling of the phagosome. It is unclear, and perhaps mainly of semantic importance, which of these four functions of proton channels is most crucial during the respiratory burst, because they occur simultaneously.

The importance of proton channel function to Nox activity has been demonstrated by the inhibition by Zn^{2+} of the production of superoxide or its product H_2O_2 in a large number of studies (90). The development of *HVCN1* knockout mice has enabled independent tests of this proposed role, which have revealed substantial, but incomplete loss of ROS production by neutrophils (88, 213), bone marrow cells (225), or B-lymphocytes (32). In support of the idea that charge compensation can be rate-limiting during Nox activity, the reduced ROS production in hH_V1 knockdown PLB-985 cells can be overcome by addition of the ionophore amphotericin B (217). Similarly, the nonselective gramicidin channel restores ROS production in mH_V1 knockout mouse neutrophils (88). Normal ROS production in a cell-free system from mH_V1 knockout mice is consistent with either charge compensation or pH regulation functions of H_V1 (225). Similarly, either mechanism could explain the restoration of ROS production by CCCP (a protonophore) in human neutrophils or eosinophils inhibited by Zn^{2+} (73, 114, 116).

Enhanced gating mode

Proton channels in phagocytes are modulated profoundly during the respiratory burst. Agonists that activate the oxidase also produce what has been called the "enhanced gating mode" of proton channels. Figure 20A illustrates the dramatic increase of H^+ currents recorded during a series of identical depolarizing pulses applied at 30-s intervals in a human eosinophil stimulated with PMA. Analyzed quantitatively (Fig. 20C), the enhanced gating response consists of a −40 mV shift of the g_H-V relationship, a 2- to 4-fold increase in maximum proton conductance ($g_{H,max}$) at large positive potentials, much faster activation kinetics (2- to 4-fold smaller τ_{act}), and much slower deactivation kinetics (2- to 6-fold larger τ_{tail}). A roughly identical constellation of changes occurs in human neutrophils (70), human eosinophils (16, 18, 37, 68), PLB-985 cells (69), murine osteoclasts (183), murine granulocytes (179), and human monocytes (194a) after stimulation with PMA or a variety of more physiological agonists including arachidonic acid (AA), fMLF, IL-5 (interleukin-5), LTB_4 (leukotriene B_4), and opsonized zymosan (which triggers phagocytosis), or during spontaneous activation by adherence to glass. The enhanced gating response occurs over several minutes with a characteristic time course (Fig. 20A and B). Although the impression is that this response is all-or-none, intermediate responses are often seen with physiological agonists like AA (37), fMLF (179), or in basophils, anti-IgE (197) whereas PMA elicits a maximal response.

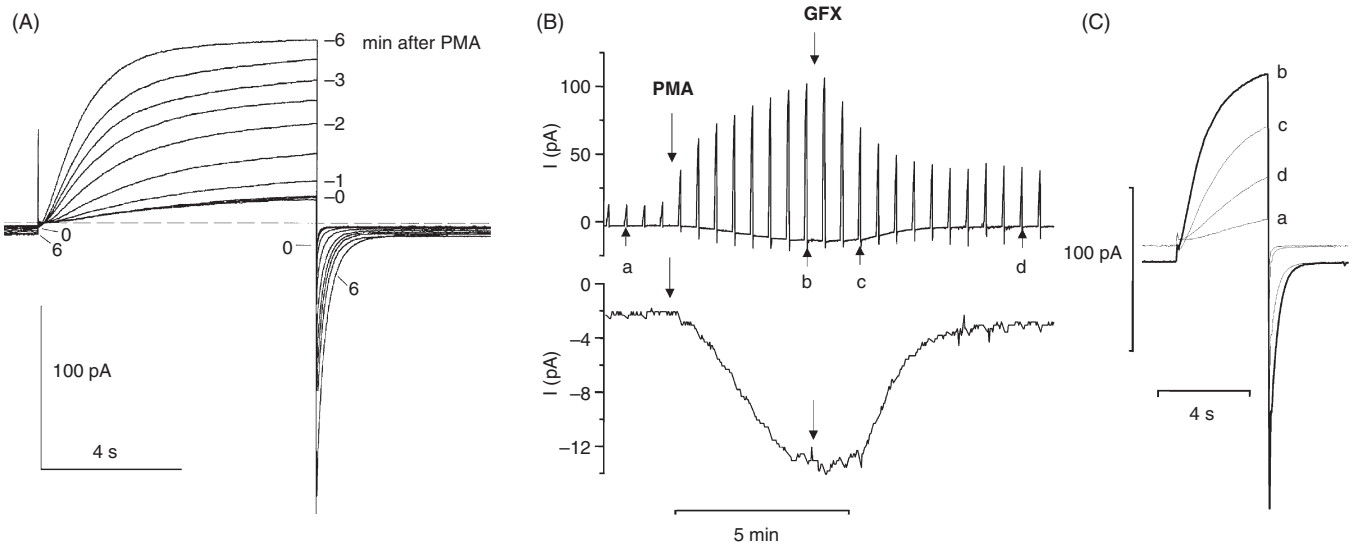

Figure 20 The enhanced gating mode of proton channels in human eosinophils. (A) The onset of enhanced gating in a human eosinophil stimulated with 30 nmol/L PMA in perforated-patch configuration at symmetrical pH 7.0. Test pulses to +60 mV applied at 30-s intervals are superimposed, before and up to 6 min after addition of PMA, illustrating the increasing current, faster activation, and slower tail current decay. The downward shift of the baseline current at −60 mV reflects electron current generated by NADPH oxidase activity. (B) The time course of proton current enhancement (top) after stimulation with PMA (arrow) and subsequent inhibition of PKC by 3 μmol/L GF109203X (GFX) (arrow) in a different human eosinophil. Repeated test pulses to +60 mV were applied, and only the peak current is evident at this time scale. The inward electron current at −60 mV in this cell can be seen as a downward deflection in the holding current, which is amplified in the lower panel (the pulses eliciting proton current are blanked). "C" shows individual currents during test pulses applied at times indicated in "B" by lower-case letters. The inward electron current at the holding potential is clearly evident. [Adapted, with permission, from reference (68). (A) Originally published in The Journal of Physiology 535: 767-781, 2001 and from reference (179) (B, C) Originally published in The Journal of Physiology 579: 327-344, 2007.]

The enhanced gating mode phenomenon is closely associated with the activation of Nox (16), and the interactions between these two molecules have not yet been completely elucidated (195). Interactions between Nox and proton channels are evident when one compares the responses of neutrophils from normal human subjects and from CGD patients. Any of several hundred specific mutations to the NADPH oxidase complex (Fig. 18) that result in loss of function produce CGD. Without medical supervision, CGD patients often die in childhood of chronic, recurrent infections (79). The first suggestion of a link between proton channels and CGD was a study showing that stimulation of CGD neutrophils with PMA failed to activate Zn^{2+} sensitive H^+ efflux through proton channels (203). Although one interpretation was that proton channels were defective, which in turn suggested that proton current was mediated by the NADPH oxidase complex itself [see Section "History"], this idea was soon disproved by a later study showing normal proton currents in these cells (204). The reason H^+ efflux did not occur in CGD cells was that without Nox activity to produce intracellular protons and membrane depolarization, there is little reason for proton channels to open. However, in later studies, the enhanced gating mode was found to differ subtly but distinctly in normal and CGD neutrophils (69). Although most of the changes characterizing enhanced gating occurred in CGD phagocytes, the negative shift of the g_H-V relationship was only half as large as in normal cells, and there was almost no slowing of deactivation (channel closing). One explanation was that a product of Nox activity modulates proton channel properties. The effects of lowering pH_i on gating are consistent with the culprit being intracellular H^+ production. Consistent with this hypothesis, enhanced gating in cells like basophils, which lack Nox activity (50), closely resembles the gestalt seen in CGD phagocytes (197).

Until recently, the final activator of proton channels in phagocytes was thought to be AA (113). Stimulation of phagocytes with PMA activates cPLA$_2\alpha$, which liberates AA (219). Although the PKC activator, PMA, produces enhanced gating of proton channels (68,69,70), AA also enhances the gating of phagocyte proton channels to a limited extent in whole-cell studies (60,105,135,239,254), but to an extent comparable to the effects of PMA in perforated-patch studies (37). Finally, cPLA$_2\alpha$ knockout mouse neutrophils or PLB-985 cells failed to exhibit Zn^{2+}-sensitive pH changes reflecting H^+ efflux (155,162,168). However, Morgan and colleagues (179) found that the enhanced gating mode elicited in cPLA$_2\alpha$ knockout mouse neutrophils stimulated with PMA or with the more physiological agonist, fMetLeuPhe, a chemotactic peptide, was indistinguishable from that seen in normal cells. Furthermore, three specific cPLA$_2\alpha$ inhibitors failed to affect the onset of enhanced gating or Nox activity (179). The prevention or reversal of some of the enhanced gating features by PKC inhibitors GF109203X [GFX, Fig. 20B, (18)] or staurosporine (179) strongly supports the idea that phosphorylation by PKC is responsible for most of the response. Finally, it was shown that when human eosinophils were stimulated by AA, the resulting enhanced gating of proton channels was partially reversed by the PKC inhibitors GF109203X or staurosporine (179). Thus, strong evidence supports the conclusion that phosphorylation of the proton channel by PKC produces enhanced gating of proton channels.

That PKC produces enhanced gating by phosphorylating the proton channel itself, not an accessory molecule, was demonstrated by a study in a B cell line, LK35.2, that does not normally exhibit proton current (194). Two candidate phosphorylation sites in the intracellular N terminus of the human proton channel (Thr^{29} and Ser^{97}) were mutated individually and together. Although both sites were detectably phosphorylated when various mutant *HVCN1* genes were expressed in LK35.2 cells, the PMA enhancement of proton currents was lost in cells expressing channels with the T29A but not the S97A mutation (194). Thus, Thr^{29} appears to be responsible for producing enhanced gating. Furthermore, at least part of the enhanced gating response is due to direct phosphorylation of the proton channel molecule.

One might wonder whether it is necessary for the enhanced gating mode to exist, given that proton channels would be activated eventually by the effects of Nox activity (depolarization and pH changes). This question was examined by Ricardo Murphy in a mathematical model of the electrical events occurring during the respiratory burst in human neutrophils and eosinophils, that was based entirely on measured parameter values (193). In the model, if proton channels were assigned their resting properties so that enhanced gating did not occur, the peak depolarization during the respiratory burst was nearly 30 mV greater. This larger depolarization reduced the Nox turnover rate calculated in eosinophils by 18% (193), due to the inhibition of electron translocation by depolarization (73). Thus, enhanced gating limits the extent of membrane depolarization, and thereby maximizes ROS production.

Histamine secretion by human basophils

Like most other leukocytes, human basophils have large voltage-gated proton currents (40). However, the best-known role of proton channels in phagocytes, namely, compensating for the electrogenic activity of Nox (see Section "The phagocyte respiratory burst") cannot apply to basophils, because these leukocytes are not phagocytic and they lack Nox (50). Nevertheless, upon stimulation with agents that trigger histamine release, including anti-IgE, fMLF, and PMA, distinct enhanced gating of proton channels was observed (197). The responses were generally smaller and more variable with the physiological agonists fMLF and anti-IgE; although only about half the cells responded, nonresponding cells were still capable of responding to PMA. Quantitative comparison of the PMA response in basophils, compared with phagocytes, revealed similarly increased $g_{H,max}$ and faster τ_{act}, but the g_H-V relationship shift was only half as large (−20 mV vs. −40 mV in phagocytes), and at most a very weak slowing of τ_{tail} was detected (197). Intriguingly, this attenuated PMA response is almost identical to that observed in human

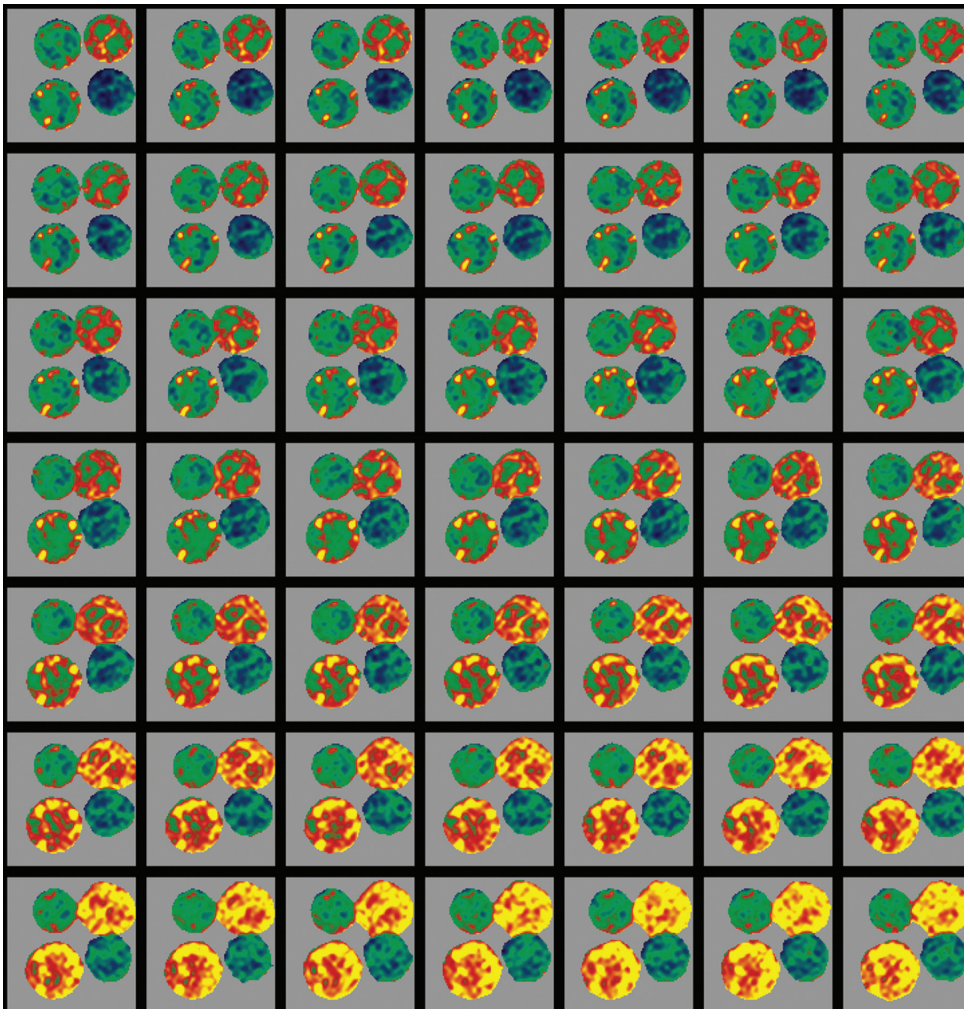

Figure 21 Confocal images of four human basophils taken at 30-s intervals (left to right, then top to bottom) during their response to anti-IgE stimulation. The pseudocolors indicate pH_i detected with SNARF-1 in confocal slices approximately 0.2 μm thick, with alkaline to acidic shown as blue to green to red to yellow. Voltage-gated proton channels are active during the response and limit the extent of acidification. (Image provided by Deri Morgan with permission.)

neutrophils from CGD patients (69) or in other leukocytes that lack significant Nox activity, such as LK35.2 cells (32). It appears that there is a mysterious functional link between proton channels and Nox that results in more profound enhancement of proton channel gating in cells that also have high levels of Nox activity (195).

That proton channels in basophils respond to agonists that trigger histamine release suggested possible involvement in this process. Zn^{2+} inhibited histamine release at concentrations that inhibit proton currents, but in a somewhat different range for PMA than for anti-IgE, consistent with these agonists acting by different signaling pathways. One might expect that proton channels might facilitate histamine release by compensating charge if Ca^{2+} influx were involved in the response, or by limiting pH_i changes. Because histamine release triggered by anti-IgE requires Ca^{2+} influx, but the responses to fMLF or PMA do not (164, 267), a general role of charge compensation seems unlikely. However, confocal imaging of pH_i using SNARF-1 revealed that basophils undergo significant acidification upon anti-IgE simulation (Fig. 21), which had not been reported previously. The acidification was exacerbated by Zn^{2+} (197), implicating proton channel activity during the response. Evidently, proton channels limit acidification during histamine release by human basophils. The step(s) in this process that are sensitive to pH_i have not yet been identified.

Do proton channels cause cancer?

A recent study reported a correlation between hH_V1 expression and the propensity for metastasis in breast cancer tissue and cell lines (266). Knockdown of hH_V1 using siRNA decreased basal pH_i and the migration of cells, suggesting that hH_V1 is constitutively active in these cells, and that hH_V1 suppression might inhibit metastasis of cancer cells. These novel results raise many questions that need to be pursued.

Conclusion

Voltage-gated proton channels are widely expressed, occurring in species ranging from unicellular dinoflagellates and coccolithophores to humans. The properties of these channels are unique, although they vary among species. They exhibit perfect proton selectivity. The protein is similar to the VSD of other voltage-gated ion channels, but it lacks an explicit pore domain. In most species, proton channels are dimers with separate conduction pathways in each protomer, but if forced, they can function as monomers. Their voltage gating mechanism in all species is exquisitely sensitive to pH_o and pH_i with the result that in multicellular species they open almost exclusively when there is an outward electrochemical gradient. The list of intriguing and diverse functions in various cells and species is growing apace. Voltage-gated proton channels trigger bioluminescence and may mediate action potentials in dinoflagellates. They promote calcification in coccolithophores. They open to extrude acid during action potentials in snail neurons. They regulate the pH in human airways and inside phagosomes. They compensate for the electrogenic activity of Nox in mammalian and human neutrophils and eosinophils. They appear to trigger maturation of human sperm. They facilitate histamine secretion by basophils. They participate in signaling cascades in human B-lymphocytes. Despite the exciting progress in recent years, many questions remain unanswered. In dozens of species, putative proton channel genes have yet to be studied. Important fundamental functions of proton channels (particularly voltage gating and pH dependence) lack mechanistic explanations. The future is positively charged.

Acknowledgements

I appreciate helpful comments on the article by Donner F. Babcock, Melania Capasso, Vladimir V. Cherny, Horst Fischer, J. Woodland Hastings, John F. Nagle, and Susan M.E. Smith. This work was supported in part by NIH grant R01-GM087507 and NSF grant MCB-0943362.

References

1. Accardi A, Miller C. Secondary active transport mediated by a prokaryotic homologue of ClC Cl^- channels. *Nature* 427: 803-807, 2004.
2. Acharya R, Carnevale V, Fiorin G, Levine BG, Polishchuk AL, Balannik V, Samish I, Lamb RA, Pinto LH, DeGrado WF, Klein ML. Structure and mechanism of proton transport through the transmembrane tetrameric M2 protein bundle of the influenza A virus. *Proc Natl Acad Sci U S A* 107: 15075-15080, 2010.
3. Agmon N. The Grotthuss mechanism. *Chem Phys Lett* 244: 456-462, 1995.
4. Agre P, King LS, Yasui M, Guggino WB, Ottersen OP, Fujiyoshi Y, Engel A, Nielsen S. Aquaporin water channels–from atomic structure to clinical medicine. *J Physiol* 542: 3-16, 2002.
5. Ahmed Z, Connor JA. Intracellular pH changes induced by calcium influx during electrical activity in molluscan neurons. *J Gen Physiol* 75: 403-426, 1980.
6. Akeson M, Deamer DW. Proton conductance by the gramicidin water wire. Model for proton conductance in the F_1F_0 ATPases? *Biophys J* 60: 101-109, 1991.
7. Alabi AA, Bahamonde MI, Jung HJ, Kim JI, Swartz KJ. Portability of paddle motif function and pharmacology in voltage sensors. *Nature* 450: 370-375, 2007.
8. Babcock DF, Pfeiffer DR. Independent elevation of cytosolic [Ca^{2+}] and pH of mammalian sperm by voltage-dependent and pH-sensitive mechanisms. *J Biol Chem* 262: 15041-15047, 1987.
9. Babcock DF, Rufo GA, Jr, Lardy HA. Potassium-dependent increases in cytosolic pH stimulate metabolism and motility of mammalian sperm. *Proc Natl Acad Sci U S A* 80: 1327-1331, 1983.
10. Babior BM, Kipnes RS, Curnutte JT. Biological defense mechanisms. The production by leukocytes of superoxide, a potential bactericidal agent. *J Clin Invest* 52: 741-744, 1973.
11. Bachvaroff TR, Place AR. From stop to start: Tandem gene arrangement, copy number and trans-splicing sites in the dinoflagellate *Amphidinium carterae*. *PLoS One* 3: e2929, 2008.
12. Baldridge CW, Gerard RW. The extra respiration of phagocytosis. *Am J Physiol* 103: 235-236, 1932.
13. Ballantine D, Abbott BC. Toxic marine flagellates; their occurrence and physiological effects on animals. *J Gen Microbiol* 16: 274-281, 1957.
14. Bánfi B, Maturana A, Jaconi S, Arnaudeau S, Laforge T, Sinha B, Ligeti E, Demaurex N, Krause KH. A mammalian H^+ channel generated through alternative splicing of the NADPH oxidase homolog NOH-1. *Science* 287: 138-142, 2000.
15. Bánfi B, Molnár G, Maturana A, Steger K, Hegedûs B, Demaurex N, Krause KH. A Ca^{2+}-activated NADPH oxidase in testis, spleen, and lymph nodes. *J Biol Chem* 276: 37594-37601, 2001.
16. Bánfi B, Schrenzel J, Nüsse O, Lew DP, Ligeti E, Krause KH, Demaurex N. A novel H^+ conductance in eosinophils: Unique characteristics and absence in chronic granulomatous disease. *J Exp Med* 190: 183-194, 1999.
17. Bankers-Fulbright JL, Gleich GJ, Kephart GM, Kita H, O'Grady SM. Regulation of eosinophil membrane depolarization during NADPH oxidase activation. *J Cell Sci* 116: 3221-3226, 2003.
18. Bankers-Fulbright JL, Kita H, Gleich GJ, O'Grady SM. Regulation of human eosinophil NADPH oxidase activity: a central role for PKCδ. *J Cell Physiol* 189: 306-315, 2001.
19. Barish ME, Baud C. A voltage-gated hydrogen ion current in the oocyte membrane of the axolotl, *Ambystoma*. *J Physiol* 352: 243-263, 1984.
20. Baud C, Barish ME. Changes in membrane hydrogen and sodium conductances during progesterone-induced maturation of *Ambystoma* oocytes. *Dev Biol* 105: 423-434, 1984.
21. Beaufort L, Probert I, de Garidel-Thoron T, Bendif EM, Ruiz-Pino D, Metzl N, Goyet C, Buchet N, Coupel P, Grelaud M, Rost B, Rickaby RE, de Vargas C. Sensitivity of coccolithophores to carbonate chemistry and ocean acidification. *Nature* 476: 80-83, 2011.
22. Bergholtz T, Daubjerg N, Moestrup Ø, Fernández-Tejedor M. On the identity of *Karlodinium veneficum* and description of *Karlodinium armiger* sp. nov. (Dinophyceae), based on light and electron microscopy, nuclear-encoded LSU rDNA, and pigment composition. *J Phycol* 42: 170-193, 2005.
23. Bernal JD, Fowler RH. A theory of water and ionic solution, with particular reference to hydrogen and hydroxyl ions. *J Chem Phys* 1: 515-548, 1933.
24. Bernheim L, Krause RM, Baroffio A, Hamann M, Kaelin A, Bader CR. A voltage-dependent proton current in cultured human skeletal muscle myotubes. *J Physiol* 470: 313-333, 1993.
25. Bode VC, Hastings JW. The purification and properties of the bioluminescent system in *Gonyaulax polyedra*. *Arch Biochem Biophys* 103: 488-499, 1963.
26. Borregaard N, Schwartz JH, Tauber AI. Proton secretion by stimulated neutrophils. Significance of hexose monophosphate shunt activity as source of electrons and protons for the respiratory burst. *J Clin Invest* 74: 455-459, 1984.
27. Brändén G, Gennis RB, Brzezinski P. Transmembrane proton translocation by cytochrome *c* oxidase. *Biochim Biophys Acta* 1757: 1052-1063, 2006.
28. Burykin A, Warshel A. What really prevents proton transport through aquaporin? Charge self-energy versus proton wire proposals. *Biophys J* 85: 3696-3706, 2003.
29. Byerly L, Meech R, Moody W, Jr Rapidly activating hydrogen ion currents in perfused neurones of the snail, *Lymnaea stagnalis*. *J Physiol* 351: 199-216, 1984.
30. Byerly L, Suen Y. Characterization of proton currents in neurones of the snail, *Lymnaea stagnalis*. *J Physiol* 413: 75-89, 1989.
31. Cameron AR, Nelson J, Forman HJ. Depolarization and increased conductance precede superoxide release by concanavalin A-stimulated rat alveolar macrophages. *Proc Natl Acad Sci U S A* 80: 3726-3728, 1983.
32. Capasso M, Bhamrah MK, Henley T, Boyd RS, Langlais C, Cain K, Dinsdale D, Pulford K, Khan M, Musset B, Cherny VV, Morgan D, Gascoyne RD, Vigorito E, DeCoursey TE, MacLennan IC, Dyer MJ. HVCN1 modulates BCR signal strength via regulation of

BCR-dependent generation of reactive oxygen species. *Nat Immunol* 11: 265-272, 2010.
33. Chakrabarti N, Tajkhorshid E, Roux B, Pomès R. Molecular basis of proton blockage in aquaporins. *Structure* 12: 65-74, 2004.
34. Chang JJ. Electrophysiological studies of a non-luminescent form of the dinoflagellate *Noctiluca miliaris*. *J Cell Comp Physiol* 56: 33-42, 1960.
35. Cheng YM, Kelly T, Church J. Potential contribution of a voltage-activated proton conductance to acid extrusion from rat hippocampal neurons. *Neuroscience* 151: 1084-1098, 2008.
36. Cherny VV, DeCoursey TE. pH-dependent inhibition of voltage-gated H^+ currents in rat alveolar epithelial cells by Zn^{2+} and other divalent cations. *J Gen Physiol* 114: 819-838, 1999.
37. Cherny VV, Henderson LM, Xu W, Thomas LL, DeCoursey TE. Activation of NADPH oxidase-related proton and electron currents in human eosinophils by arachidonic acid. *J Physiol* 535: 783-794, 2001.
38. Cherny VV, Markin VS, DeCoursey TE. The voltage-activated hydrogen ion conductance in rat alveolar epithelial cells is determined by the pH gradient. *J Gen Physiol* 105: 861-896, 1995.
39. Cherny VV, Murphy R, Sokolov V, Levis RA, DeCoursey TE. Properties of single voltage-gated proton channels in human eosinophils estimated by noise analysis and by direct measurement. *J Gen Physiol* 121: 615-628, 2003.
40. Cherny VV, Thomas LL, DeCoursey TE. Voltage-gated proton currents in human basophils. *Biol Membrany* 18: 458-465, 2001.
41. Chernyshev A, Cukierman S. Thermodynamic view of activation energies of proton transfer in various gramicidin A channels. *Biophys J* 82: 182-192, 2002.
42. Chernyshev A, Pomès R, Cukierman S. Kinetic isotope effects of proton transfer in aqueous and methanol containing solutions, and in gramicidin A channels. *Biophys Chem* 103: 179-190, 2003.
43. Chizhmakov IV, Geraghty FM, Ogden DC, Hayhurst A, Antoniou M, Hay AJ. Selective proton permeability and pH regulation of the influenza virus M2 channel expressed in mouse erythroleukaemia cells. *J Physiol* 494: 329-336, 1996.
44. Cho DY, Hajighasemi M, Hwang PH, Illek B, Fischer H. Proton secretion in freshly excised sinonasal mucosa from asthma and sinusitis patients. *Am J Rhinol Allergy* 23: e10-e13, 2009.
45. Cohen HJ, Newburger PE, Chovaniec ME, Whitin JC, Simons ER. Opsonized zymosan-stimulated granulocytes-activation and activity of the superoxide-generating system and membrane potential changes. *Blood* 58: 975-982, 1981.
46. Cole KS, Moore JW. Potassium ion current in the squid giant axon: Dynamic characteristic. *Biophys J* 1: 1-14, 1960.
47. Conway BE, Bockris JOM, Linton H. Proton conductance and the existence of the $H_3O^{\cdot}$ ion. *J Chem Phys* 24: 834-850, 1956.
48. Cukierman S. Flying protons in linked gramicidin A channels. *Israel J Chem* 39: 419-426, 1999.
49. Danneel H. Notiz über Ionengeschwindigkeiten. *Z Elktrochem Angew P* 11: 249-252, 1905.
50. de Boer M, Roos D. Metabolic comparison between basophils and other leukocytes from human blood. *J Immunol* 136: 3447-3454, 1986.
51. de Groot BL, Frigato T, Helms V, Grubmüller H. The mechanism of proton exclusion in the aquaporin-1 water channel. *J Mol Biol* 333: 279-293, 2003.
52. de Grotthuss CJ. Memoir on the decomposition of water and of the bodies that it holds in solution by means of galvanic electricity. *Biochim Biophys Acta* 1757: 871-875, 2006.
53. de Grotthuss CJT. Sur la décomposition de l'eau et des corps qu'elle tient en dissolution à l'aide de l'électricité galvanique. *Annales de Chimie LVIII*: 54-74, 1806.
54. DeCoursey TE. Hydrogen ion currents in rat alveolar epithelial cells. *Biophys J* 60: 1243-1253, 1991.
55. DeCoursey TE. Hypothesis: Do voltage-gated H^+ channels in alveolar epithelial cells contribute to CO_2 elimination by the lung? *Am J Physiol Cell Physiol* 278: C1-C10, 2000.
56. DeCoursey TE. Voltage-gated proton channels and other proton transfer pathways. *Physiol Rev* 83: 475-579, 2003.
57. DeCoursey TE. Voltage-gated proton channels: What's next? *J Physiol* 586: 5305-5324, 2008.
58. DeCoursey TE. Voltage-gated proton channels find their dream job managing the respiratory burst in phagocytes. *Physiology (Bethesda)* 25: 27-40, 2010.
59. DeCoursey TE, Chandy KG, Gupta S, Cahalan MD. Voltage-gated K^+ channels in human T lymphocytes: A role in mitogenesis? *Nature* 307: 465-468, 1984.
60. DeCoursey TE, Cherny VV. Potential, pH, and arachidonate gate hydrogen ion currents in human neutrophils. *Biophys J* 65: 1590-1598, 1993.
61. DeCoursey TE, Cherny VV. Na^+-H^+ antiport detected through hydrogen ion currents in rat alveolar epithelial cells and human neutrophils. *J Gen Physiol* 103: 755-785, 1994.
62. DeCoursey TE, Cherny VV. Voltage-activated hydrogen ion currents. *J Membr Biol* 141: 203-223, 1994.
63. DeCoursey TE, Cherny VV. Voltage-activated proton currents in membrane patches of rat alveolar epithelial cells. *J Physiol* 489: 299-307, 1995.
64. DeCoursey TE, Cherny VV. Effects of buffer concentration on voltage-gated H^+ currents: Does diffusion limit the conductance? *Biophys J* 71: 182-193, 1996.
65. DeCoursey TE, Cherny VV. Voltage-activated proton currents in human THP-1 monocytes. *J Membr Biol* 152: 131-140, 1996.
66. DeCoursey TE, Cherny VV. Deuterium isotope effects on permeation and gating of proton channels in rat alveolar epithelium. *J Gen Physiol* 109: 415-434, 1997.
67. DeCoursey TE, Cherny VV. Temperature dependence of voltage-gated H^+ currents in human neutrophils, rat alveolar epithelial cells, and mammalian phagocytes. *J Gen Physiol* 112: 503-522, 1998.
68. DeCoursey TE, Cherny VV, DeCoursey AG, Xu W, Thomas LL. Interactions between NADPH oxidase-related proton and electron currents in human eosinophils. *J Physiol* 535: 767-781, 2001.
69. DeCoursey TE, Cherny VV, Morgan D, Katz BZ, Dinauer MC. The $gp91^{phox}$ component of NADPH oxidase is not the voltage-gated proton channel in phagocytes, but it helps. *J Biol Chem* 276: 36063-36066, 2001.
70. DeCoursey TE, Cherny VV, Zhou W, Thomas LL. Simultaneous activation of NADPH oxidase-related proton and electron currents in human neutrophils. *Proc Natl Acad Sci U S A* 97: 6885-6889, 2000.
71. DeCoursey TE, Jacobs ER, Silver MR. Potassium currents in rat type II alveolar epithelial cells. *J Physiol* 395: 487-505, 1988.
72. DeCoursey TE, Ligeti E. Regulation and termination of NADPH oxidase activity. *Cell Mol Life Sci* 62: 2173-2193, 2005.
73. DeCoursey TE, Morgan D, Cherny VV. The voltage dependence of NADPH oxidase reveals why phagocytes need proton channels. *Nature* 422: 531-534, 2003.
74. Deeds JR, Terlizzi DE, Adolf JE, Stoecker DK, Place AR. Toxic activity from cultures of *Karlodinium micrum* (=*Gyrodinium galatheanum*)(Dinophyceae)-a dinoflagellate associated with fish mortalities in an estuarine aquaculture facility. *Harmful Algae* 1: 169-189, 2002.
75. Demaurex N, Downey GP, Waddell TK, Grinstein S. Intracellular pH regulation during spreading of human neutrophils. *J Cell Biol* 133: 1391-1402, 1996.
76. Demaurex N, Grinstein S, Jaconi M, Schlegel W, Lew DP, Krause KH. Proton currents in human granulocytes: Regulation by membrane potential and intracellular pH. *J Physiol* 466: 329-344, 1993.
77. Demaurex N, Petheõ GL. Electron and proton transport by NADPH oxidases. *Philos Trans R Soc Lond B Biol Sci* 360: 2315-2325, 2005.
78. DeSa R, Hastings JW. The characterization of scintillons. Bioluminescent particles from the marine dinoflagellate, *Gonyaulax polyedra*. *J Gen Physiol* 51: 105-122, 1968.
79. Dinauer MC, Nauseef WM, Newburger PEI. Inherited disorders of oxidative phagocyte killing. In: Scriver CR, Beaudet AL, Sly WS, Valle D, editors. *The Metabolic and Molecular Bases of Inherited Disease*. 8th ed. http://www.ommbid.com/, New York, McGraw-Hill, 2001, Chap.189. New York: McGraw-Hill Inc, Updated October, 2009.
80. Eckert R. Excitation and luminescence in *Noctiluca miliaris*. In: Johnson FH, Haneda Y, editors *Bioluminescence in Progress*, Princeton, NJ: Princeton University Press, 1966, p. 269-300.
81. Eckert R. II. Asynchronous flash initiation by a propagated triggering potential. *Science* 147: 1142-1145, 1965.
82. Eckert R, Reynolds GT. The subcellular origin of bioluminescence in *Noctiluca miliaris*. *J Gen Physiol* 50: 1429-1458, 1967.
83. Eckert R, Sibaoka T. The flash-triggering action potential of the luminescent dinoflagellate *Noctiluca*. *J Gen Physiol* 52: 258-282, 1968.
84. Effros RM, Mason G, Silverman P. Asymmetric distribution of carbonic anhydrase in the alveolar-capillary barrier. *J Appl Physiol* 51: 190-193, 1981.
85. Effros RM, Olson L, Lin W, Audi S, Hogan G, Shaker R, Hoagland K, Foss B. Resistance of the pulmonary epithelium to movement of buffer ions. *Am J Physiol Lung Cell Mol Physiol* 285: L476-L483, 2003.
86. Eigen M, De Maeyer L. Self-dissociation and protonic charge transport in water and ice. *Proc R Soc Lond A* 247: 505-533, 1958.
87. El Chemaly A, Guinamard R, Demion M, Fares N, Jebara V, Faivre JF, Bois P. A voltage-activated proton current in human cardiac fibroblasts. *Biochem Biophys Res Commun* 340: 512-516, 2006.
88. El Chemaly A, Okochi Y, Sasaki M, Arnaudeau S, Okamura Y, Demaurex N. VSOP/Hv1 proton channels sustain calcium entry, neutrophil migration, and superoxide production by limiting cell depolarization and acidification. *J Exp Med* 207: 129-139, 2010.
89. Elinder F, Århem P. Metal ion effects on ion channel gating. *Q Rev Biophys* 36: 373-427, 2004.
90. Femling JK, Cherny VV, Morgan D, Rada B, Davis AP, Czirják G, Enyedi P, England SK, Moreland JG, Ligeti E, Nauseef WM, DeCoursey TE. The antibacterial activity of human neutrophils and

eosinophils requires proton channels but not BK channels. *J Gen Physiol* 127: 659-672, 2006.
91. Fischer H. Function of proton channels in lung epithelia. *WIREs Membr Transp Signal* 2011. doi: 10.1002/wmts.17 (In press)
92. Fischer H, Gonzales LK, Kolla V, Schwarzer C, Miot F, Illek B, Ballard PL. Developmental regulation of DUOX1 expression and function in human fetal lung epithelial cells. *Am J Physiol Lung Cell Mol Physiol* 292: L1506-L1514, 2007.
93. Fischer H, Widdicombe JH. Mechanisms of acid and base secretion by the airway epithelium. *J Membr Biol* 211: 139-150, 2006.
94. Fischer H, Widdicombe JH, Illek B. Acid secretion and proton conductance in human airway epithelium. *Am J Physiol Cell Physiol* 282: C736-743, 2002.
95. Fogel M Hastings JW. A substrate-binding protein in the *Gonyaulax* bioluminescence reaction. *Arch Biochem Biophys* 142: 310-321, 1971.
96. Fogel M, Hastings JW. Bioluminescence: Mechanism and mode of control of scintillon activity. *Proc Natl Acad Sci U S A* 69: 690-693, 1972.
97. Forteza R, Salathe M, Miot F, Forteza R, Conner GE. Regulated hydrogen peroxide production by Duox in human airway epithelial cells. *Am J Respir Cell Mol Biol* 32: 462-469, 2005.
98. Frankenhaeuser B, Hodgkin AL. The action of calcium on the electrical properties of squid axons. *J Physiol* 137: 218-244, 1957.
99. Fujiwara Y, Kurokawa T, Takeshita K, Kobayashi M, Nakagawa A, Okamura Y. Stability of the cytoplasmic dimer assembly regulates the thermosensitive gating of the voltage-gated H^+ channel. *Biophys J* 100: 348a, 2011.
100. Geiszt M, Kapus A, Nemet K, Farkas L, Ligeti E. Regulation of capacitative Ca^{2+} influx in human neutrophil granulocytes. Alterations in chronic granulomatous disease. *J Biol Chem* 272: 26471-26478, 1997.
101. Gilly WF, Armstrong CM. Divalent cations and the activation kinetics of potassium channels in squid giant axons. *J Gen Physiol* 79: 965-996, 1982.
102. Goldman DE. Potential, impedance, and rectification in membranes. *J Gen Physiol* 27: 37-60, 1943.
103. Gonzalez C, Koch HP, Drum BM, Larsson HP. Strong cooperativity between subunits in voltage-gated proton channels. *Nat Struct Mol Biol* 17: 51-56, 2010.
104. Gonzalez C, Rebolledo S, Wang X, Perez M, Larsson HP. Contribution of S4 charges to gating mechanism in Hv channels. *Biophys J* 100: 173a, 2011.
105. Gordienko DV, Tare M, Parveen S, Fenech CJ, Robinson C, Bolton TB. Voltage-activated proton current in eosinophils from human blood. *J Physiol* 496: 299-316, 1996.
106. Hamill OP, Marty A, Neher E, Sakmann B, Sigworth FJ. Improved patch-clamp techniques for high-resolution current recording from cells and cell-free membrane patches. *Pflügers Arch* 391: 85-100, 1981.
107. Hampton MB, Kettle AJ, Winterbourn CC. Inside the neutrophil phagosome: Oxidants, myeloperoxidase, and bacterial killing. *Blood* 92: 3007-3017, 1998.
108. Hanke W, Miller C. Single chloride channels from *Torpedo* electroplax. Activation by protons. *J Gen Physiol* 82: 25-45, 1983.
109. Hastings JW. Bacterial and dinoflagellate luminescent systems. In: Herring P, editor. *Bioluminescence in Action*, London: Academic Press, 1978, p. 129-170.
110. Hastings JW. Bioluminescence. In: Sperelakis N, editor. *Cell Physiology Sourcebook: A Molecular Approach* (3rd ed), San Diego: Academic Press, 2001, p. 1115-1131.
111. Hastings JW, Vergin M, DeSa R. Scintillons: The biochemistry of dinoflagellate bioluminescence. In: Johnson FH, Haneda Y, editors. *Bioluminescence in Progress*, Princeton NJ: Princeton University Press, 1966, p. 301-329.
112. Henderson LM, Banting G, Chappell JB. The arachidonate-activable, NADPH oxidase-associated H^+ channel. Evidence that gp91-*phox* functions as an essential part of the channel. *J Biol Chem* 270: 5909-5916, 1995.
113. Henderson LM, Chappell JB. The NADPH-oxidase-associated H^+ channel is opened by arachidonate. *Biochem J* 283: 171-175, 1992.
114. Henderson LM, Chappell JB, Jones OTG. The superoxide-generating NADPH oxidase of human neutrophils is electrogenic and associated with an H^+ channel. *Biochem J* 246: 325-329, 1987.
115. Henderson LM, Chappell JB, Jones OTG. Internal pH changes associated with the activity of NADPH oxidase of human neutrophils. Further evidence for the presence of an H^+ conducting channel. *Biochem J* 251: 563-567, 1988.
116. Henderson LM, Chappell JB, Jones OTG. Superoxide generation by the electrogenic NADPH oxidase of human neutrophils is limited by the movement of a compensating charge. *Biochem J* 255: 285-290, 1988.
117. Henderson LM, Meech RW. Evidence that the product of the human X-linked CGD gene, gp91-*phox*, is a voltage-gated H^+ pathway. *J Gen Physiol* 114: 771-786, 1999.
118. Henderson LM, Thomas S, Banting G, Chappell JB. The arachidonate-activatable, NADPH oxidase-associated H^+ channel is contained within the multi-membrane-spanning N-terminal region of gp91-*phox*. *Biochem J* 325: 701-705, 1997.
119. Hille B. *Ion Channels of Excitable Membranes*. Sunderland, MA: Sinauer Associates, Inc, 2001.
120. Hisada M. Membrane resting and action potentials from a protozoan, *Noctiluca scintillans*. *J Cell Comp Physiol* 50: 57-71, 1957.
121. Hodgkin AL, Huxley AF. The dual effect of membrane potential on sodium conductance in the giant axon of *Loligo*. *J Physiol* 116: 497-506, 1952.
122. Hodgkin AL, Huxley AF. A quantitative description of membrane current and its application to conduction and excitation in nerve. *J Physiol* 117: 500-544, 1952.
123. Hodgkin AL, Katz B. The effect of sodium ions on the electrical activity of giant axon of the squid. *J Physiol* 108: 37-77, 1949.
124. Hu F, Luo W, Hong M. Mechanisms of proton conduction and gating in influenza M2 proton channels from solid-state NMR. *Science* 330: 505-508, 2010.
125. Humez S, Collin T, Matifat F, Guilbault P, Fournier F. $InsP_3$-dependent Ca^{2+} oscillations linked to activation of voltage-dependent H^+ conductance in *Rana esculenta* oocytes. *Cell Signal* 8: 375-379, 1996.
126. Humez S, Fournier F, Guilbault P. A voltage-dependent and pH-sensitive proton current in *Rana esculenta* oocytes. *J Membr Biol* 147: 207-215, 1995.
127. Ilan B, Tajkhorshid E, Schulten K, Voth GA. The mechanism of proton exclusion in aquaporin channels. *Proteins* 55: 223-228, 2004.
128. Iovannisci D, Illek B, Fischer H. Function of the HVCN1 proton channel in airway epithelia and a naturally occurring mutation, M91T. *J Gen Physiol* 136: 35-46, 2010.
129. Iyer GYN, Islam MF, Quastel JH. Biochemical aspects of phagocytosis. *Nature* 192: 535-541, 1961.
130. Jankowski A, Grinstein S. A noninvasive fluorimetric procedure for measurement of membrane potential. Quantification of the NADPH oxidase-induced depolarization in activated neutrophils. *J Biol Chem* 274: 26098-26104, 1999.
131. Jiang Y, Lee A, Chen J, Ruta V, Cadene M, Chait BT, MacKinnon R. X-ray structure of a voltage-dependent K^+ channel. *Nature* 423: 33-41, 2003.
132. Jones GS, VanDyke K, Castranova V. Transmembrane potential changes associated with superoxide release from human granulocytes. *J Cell Physiol* 106: 75-83, 1981.
133. Joseph D, Tirmizi O, Zhang XL, Crandall ED, Lubman RL. Polarity of alveolar epithelial cell acid-base permeability. *Am J Physiol Lung Cell Mol Physiol* 282: L675-683, 2002.
134. Kapus A, Romanek R, Qu AY, Rotstein OD, Grinstein S. A pH-sensitive and voltage-dependent proton conductance in the plasma membrane of macrophages. *J Gen Physiol* 102: 729-760, 1993.
135. Kapus A, Szuszták K, Ligeti E. Regulation of the electrogenic H^+ channel in the plasma membrane of neutrophils: possible role of phospholipase A_2, internal and external protons. *Biochem J* 292: 445-450, 1993.
136. Kass I, Arkin IT. How pH opens a H^+ channel: The gating mechanism of influenza A M2. *Structure* 13: 1789-1798, 2005.
137. Khurana E, Dal Peraro M, DeVane R, Vemparala S, DeGrado WF, Klein ML. Molecular dynamics calculations suggest a conduction mechanism for the M2 proton channel from influenza A virus. *Proc Natl Acad Sci U S A* 106: 1069-1074, 2009.
138. Klebanoff SJ. Myeloperoxidase: contribution to the microbicidal activity of intact leukocytes. *Science* 169: 1095-1097, 1970.
139. Koch HP, Kurokawa T, Okochi Y, Sasaki M, Okamura Y, Larsson HP. Multimeric nature of voltage-gated proton channels. *Proc Natl Acad Sci U S A* 105: 9111-9116, 2008.
140. Korchak HM, Weissmann G. Changes in membrane potential of human granulocytes antecede the metabolic responses to surface stimulation. *Proc Natl Acad Sci U S A* 75: 3818-3822, 1978.
141. Krieger N, Hastings JW. Bioluminescence: pH activity profiles of related luciferase fractions. *Science* 161: 586-589, 1968.
142. Kukol A, Adams PD, Rice LM, Brunger AT, Arkin TI. Experimentally based orientational refinement of membrane protein models: A structure for the *Influenza* A M2 H^+ channel. *J Mol Biol* 286: 951-962, 1999.
143. Kumánovics A, Levin G, Blount P. Family ties of gated pores: Evolution of the sensor module. *Faseb J* 16: 1623-1629, 2002.
144. Kuno M, Ando H, Morihata H, Sakai H, Mori H, Sawada M, Oiki S. Temperature dependence of proton permeation through a voltage-gated proton channel. *J Gen Physiol* 134: 191-205, 2009.
145. Kuno M, Kawawaki J, Nakamura F. A highly temperature-sensitive proton current in mouse bone marrow-derived mast cells. *J Gen Physiol* 109: 731-740, 1997.
146. Laggner H, Phillipp K, Goldenberg H. Free zinc inhibits transport of vitamin C in differentiated HL-60 cells during respiratory burst. *Free Radic Biol Med* 40: 436-443, 2006.

147. Larsson HP, Baker OS, Dhillon DS, Isacoff EY. Transmembrane movement of the shaker K^+ channel S4. *Neuron* 16: 387-397, 1996.
148. Lear JD. Proton conduction through the M2 protein of the influenza A virus; a quantitative, mechanistic analysis of experimental data. *FEBS Lett* 552: 17-22, 2003.
149. Lee SC, Steinhardt RA. pH changes associated with meiotic maturation in oocytes of *Xenopus laevis*. *Dev Biol* 85: 358-369, 1981.
150. Lee SY, Letts JA, Mackinnon R. Dimeric subunit stoichiometry of the human voltage-dependent proton channel Hv1. *Proc Natl Acad Sci U S A* 105: 7692-7695, 2008.
151. Lee SY, Letts JA, MacKinnon R. Functional reconstitution of purified human Hv1 H^+ channels. *J Mol Biol* 387: 1055-1060, 2009.
152. Leiding T, Wang J, Martinsson J, DeGrado WF, Årsköld SP. Proton and cation transport activity of the M2 proton channel from influenza A virus. *Proc Natl Acad Sci U S A* 107: 15409-15414, 2010.
153. Levis RA, Rae JL. The use of quartz patch pipettes for low noise single channel recording. *Biophys J* 65: 1666-1677, 1993.
154. Levitt DG, Elias SR, Hautman JM. Number of water molecules coupled to the transport of sodium, potassium and hydrogen ions via gramicidin, nonactin or valinomycin. *Biochim Biophys Acta* 512: 436-451, 1978.
155. Levy R, Lowenthal A, Dana R. Cytosolic phospholipase A_2 is required for the activation of the NADPH oxidase associated H^+ channel in phagocyte-like cells. *Adv Exp Med Biol* 479: 125-135, 2000.
156. Li SJ, Zhao Q, Zhou Q, Unno H, Zhai Y, Sun F. The role and structure of the carboxyl-terminal domain of the human voltage-gated proton channel Hv1. *J Biol Chem* 285: 12047-12054, 2010.
157. Lin MC, Hsieh JY, Mock AF, Papazian DM. R1 in the Shaker S4 occupies the gating charge transfer center in the resting state. *J Gen Physiol* 138: 155-163.
158. Lin TI, Schroeder C. Definitive assignment of proton selectivity and attoampere unitary current to the M2 ion channel protein of influenza a virus. *J Virol* 75: 3647-3656, 2001.
159. Lisal J, Maduke M. The ClC-0 chloride channel is a 'broken' Cl^-/H^+ antiporter. *Nat Struct Mol Biol* 15: 805-810, 2008.
160. Lishko PV, Botchkina IL, Fedorenko A, Kirichok Y. Acid extrusion from human spermatozoa is mediated by flagellar voltage-gated proton channel. *Cell* 140: 327-337, 2010.
161. Long SB, Tao X, Campbell EB, MacKinnon R. Atomic structure of a voltage-dependent K^+ channel in a lipid membrane-like environment. *Nature* 450: 376-382, 2007.
162. Lowenthal A, Levy R. Essential requirement of cytosolic phospholipase A_2 for activation of the H^+ channel in phagocyte-like cells. *J Biol Chem* 274: 21603-21608, 1999.
163. Ludewig U, Pusch M, Jentsch TJ. Two physically distinct pores in the dimeric ClC-0 chloride channel. *Nature* 383: 340-343, 1996.
164. MacGlashan D, Jr. Botana LM. Biphasic Ca^{2+} responses in human basophils. Evidence that the initial transient elevation associated with the mobilization of intracellular calcium is an insufficient signal for degranulation. *J Immunol* 150: 980-991, 1993.
165. Magneson GR, Puvathingal JM, Ray WJ, Jr. The concentrations of free Mg^{2+} and free Zn^{2+} in equine blood plasma. *J Biol Chem* 262: 11140-11148, 1987.
166. Mahaut-Smith MP. The effect of zinc on calcium and hydrogen ion currents in intact snail neurones. *J Exp Biol* 145: 455-464, 1989.
167. Mahaut-Smith MP. Separation of hydrogen ion currents in intact molluscan neurones. *J Exp Biol* 145: 439-454, 1989.
168. Mankelow TJ, Pessach E, Levy R, Henderson LM. The requirement of cytosolic phospholipase A_2 for the PMA activation of proton efflux through the N-terminal 230-amino-acid fragment of $gp91^{phox}$. *Biochem J* 374: 315-319, 2003.
169. Maturana A, Arnaudeau S, Ryser S, Banfi B, Hossle JP, Schlegel W, Krause KH, Demaurex N. Heme histidine ligands within $gp91^{phox}$ modulate proton conduction by the phagocyte NADPH oxidase. *J Biol Chem* 276: 30277-30284, 2001.
170. Meech RW, Thomas RC. Voltage-dependent intracellular pH in *Helix aspersa* neurones. *J Physiol* 390: 433-452, 1987.
171. Middleton RE, Pheasant DJ, Miller C. Homodimeric architecture of a ClC-type chloride ion channel. *Nature* 383: 337-340, 1996.
172. Miller C. ClC chloride channels viewed through a transporter lens. *Nature* 440: 484-489, 2006.
173. Miller C. Lonely voltage sensor seeks protons for permeation. *Science* 312: 534-535, 2006.
174. Miller C, White MM. A voltage-dependent chloride conductance channel from *Torpedo* electroplax membrane. *Ann N Y Acad Sci* 341: 534-551, 1980.
175. Miloshevsky GV, Jordan PC. Water and ion permeation in bAQP1 and GlpF channels: A kinetic Monte Carlo study. *Biophys J* 87: 3690-3702, 2004.
176. Minor DL, Jr. A sensitive channel family replete with sense and motion. *Nat Struct Mol Biol* 13: 388-390, 2006.
177. Mitchell P. Coupling of phosphorylation to electron and hydrogen transfer by a chemi-osmotic type of mechanism. *Nature* 191: 144-148, 1961.
178. Morgan D, Capasso M, Musset B, Cherny VV, Ríos E, Dyer MJS, DeCoursey TE. Voltage-gated proton channels maintain pH in human neutrophils during phagocytosis. *Proc Natl Acad Sci U S A* 106: 18022-18027, 2009.
179. Morgan D, Cherny VV, Finnegan A, Bollinger J, Gelb MH, DeCoursey TE. Sustained activation of proton channels and NADPH oxidase in human eosinophils and murine granulocytes requires PKC but not $cPLA_2\alpha$ activity. *J Physiol* 579: 327-344, 2007.
180. Morgan D, Cherny VV, Murphy R, Katz BZ, DeCoursey TE. The pH dependence of NADPH oxidase in human eosinophils. *J Physiol* 569: 419-431, 2005.
181. Morgan D, Cherny VV, Price MO, Dinauer MC, DeCoursey TE. Absence of proton channels in COS-7 cells expressing functional NADPH oxidase components. *J Gen Physiol* 119: 571-580, 2002.
182. Morgan D, DeCoursey TE. Simultaneous measurement of phagosome and plasma membrane potentials in human neutrophils by di-8-Anepps and SEER. *Biophys J* 96: 55a, 2010.
183. Mori H, Sakai H, Morihata H, Kawawaki J, Amano H, Yamano T, Kuno M. Regulatory mechanisms and physiological relevance of a voltage-gated H^+ channel in murine osteoclasts: Phorbol myristate acetate induces cell acidosis and the channel activation. *J Bone Miner Res* 18: 2069-2076, 2003.
184. Mori H, Sakai H, Morihata H, Yamano T, Kuno M. A voltage-gated H^+ channel is a powerful mechanism for pH homeostasis in murine osteoclasts. *Kobe J Med Sci* 48: 87-96, 2002.
185. Morihata H, Kawawaki J, Okina M, Sakai H, Notomi T, Sawada M, Kuno M. Early and late activation of the voltage-gated proton channel during lactic acidosis through pH-dependent and -independent mechanisms. *Pflügers Arch* 455: 829-838, 2008.
186. Morihata H, Kawawaki J, Sakai H, Sawada M, Tsutada T, Kuno M. Temporal fluctuations of voltage-gated proton currents in rat spinal microglia via pH-dependent and -independent mechanisms. *Neurosci Res* 38: 265-271, 2000.
187. Morihata H, Nakamura F, Tsutada T, Kuno M. Potentiation of a voltage-gated proton current in acidosis-induced swelling of rat microglia. *J Neurosci* 20: 7220-7227, 2000.
188. Moskwa P, Lorentzen D, Excoffon KJ, Zabner J, McCray PB, Jr, Nauseef WM, Dupuy C, Bánfi B. A novel host defense system of airways is defective in cystic fibrosis. *Am J Respir Crit Care Med* 175: 174-183, 2007.
189. Mould JA, Li HC, Dudlak CS, Lear JD, Pekosz A, Lamb RA, Pinto LH. Mechanism for proton conduction of the M_2 ion channel of influenza A virus. *J Biol Chem* 275: 8592-8599, 2000.
190. Murata K, Mitsuoka K, Hirai T, Walz T, Agre P, Heymann JB, Engel A, Fujiyoshi Y. Structural determinants of water permeation through aquaporin-1. *Nature* 407: 599-605, 2000.
191. Murata Y, Iwasaki H, Sasaki M, Inaba K, Okamura Y. Phosphoinositide phosphatase activity coupled to an intrinsic voltage sensor. *Nature* 435: 1239-1243, 2005.
192. Murphy R, Cherny VV, Morgan D, DeCoursey TE. Voltage-gated proton channels help regulate pH_i in rat alveolar epithelium. *Am J Physiol Lung Cell Mol Physiol* 288: L398-L408, 2005.
193. Murphy R, DeCoursey TE. Charge compensation during the phagocyte respiratory burst. *Biochim Biophys Acta* 1757: 996-1011, 2006.
194. Musset B, Capasso M, Cherny VV, Morgan D, Bhamrah M, Dyer MJS, DeCoursey TE. Identification of Thr^{29} as a critical phosphorylation site that activates the human proton channel *Hvcn1* in leukocytes. *J Biol Chem* 285: 5117-5121, 2010.
194a. Musset B, Cherny VV, DeCoursey TE. Strong glucose dependence of electron current in human monocytes. *Am J Physiol: Cell Physiol* (In press).
195. Musset B, Cherny VV, Morgan D, DeCoursey TE. The intimate and mysterious relationship between proton channels and NADPH oxidase. *FEBS Lett* 583: 7-12, 2009.
196. Musset B, Cherny VV, Morgan D, Okamura Y, Ramsey IS, Clapham DE, DeCoursey TE. Detailed comparison of expressed and native voltage-gated proton channel currents. *J Physiol* 586: 2477-2486, 2008.
197. Musset B, Morgan D, Cherny VV, MacGlashan DW, Jr, Thomas LL, Ríos E, DeCoursey TE. A pH-stabilizing role of voltage-gated proton channels in IgE-mediated activation of human basophils. *Proc Natl Acad Sci U S A* 105: 11020-11025, 2008.
198. Musset B, Smith SM, Rajan S, Cherny VV, Morgan D, DeCoursey TE. Oligomerization of the voltage gated proton channel. *Channels (Austin)* 4: 260-265, 2010.
199. Musset B, Smith SM, Rajan S, Cherny VV, Sujai S, Morgan D, DeCoursey TE. Zinc inhibition of monomeric and dimeric proton channels suggests cooperative gating. *J Physiol* 588: 1435-1449, 2010.
200. Musset B, Smith SME, Rajan S, Morgan D, Cherny VV, DeCoursey TE. $Aspartate^{112}$ is the selectivity filter of the human voltage gated proton channel. *Nature* doi: 10.1038/nature10557, 2011.

201. Myers VB, Haydon DA. Ion transfer across lipid membranes in the presence of gramicidin A: The ion selectivity. *Biochim Biophys Acta* 274: 313-322, 1972.
202. Nagle JF Morowitz HJ. Molecular mechanisms for proton transport in membranes. *Proc Natl Acad Sci U S A* 75: 298-302, 1978.
203. Nanda A, Grinstein S, Curnutte JT. Abnormal activation of H^+ conductance in NADPH oxidase-defective neutrophils. *Proc Natl Acad Sci U S A* 90: 760-764, 1993.
204. Nanda A, Romanek R, Curnutte JT, Grinstein S. Assessment of the contribution of the cytochrome *b* moiety of the NADPH oxidase to the transmembrane H^+ conductance of leukocytes. *J Biol Chem* 269: 27280-27285, 1994.
205. Nawata T, Sibaoka T. Ionic composition and pH of the vacuolar sap in marine dinoflagellate *Noctiluca*. *Plant Cell Physiol* 17: 265-272, 1976.
206. Nawata T Sibaoka T. Coupling between action potential and bioluminescence in *Noctiluca*: Effects of inorganic ions and pH in vacuolar sap. *J Comp Physiol* 134: 137-149, 1979.
207. Nelson RD, Kuan G, Saier MH, Jr, Montal M. Modular assembly of voltage-gated channel proteins: A sequence analysis and phylogenetic study. *J Mol Microbiol Biotechnol* 1: 281-287, 1999.
208. Ng AW, Bidani A, Heming TA. Innate host defense of the lung: effects of lung-lining fluid pH. *Lung* 182: 297-317, 2004.
209. Nicolas MT, Sweeney BM, Hastings JW. The ultrastructural localization of luciferase in three bioluminescent dinoflagellates, two species of *Pyrocystis*, and *Noctiluca*, using anti-luciferase and immunogold labelling. *J Cell Sci* 87: 189-196, 1987.
210. Nielson DW, Goerke J, Clements JA. Alveolar subphase pH in the lungs of anesthetized rabbits. *Proc Natl Acad Sci U S A* 78: 7119-7123, 1981.
211. Nordström T, Rotstein OD, Romanek R, Asotra S, Heersche JN, Manolson MF, Brisseau GF, Grinstein S. Regulation of cytoplasmic pH in osteoclasts. Contribution of proton pumps and a proton-selective conductance. *J Biol Chem* 270: 2203-2212, 1995.
212. Oami K. Correlation between membrane potential responses and tentacle movement in the dinoflagellate *Noctiluca miliaris*. *Zoolog Sci* 21: 131-138, 2004.
213. Okochi Y, Sasaki M, Iwasaki H, Okamura Y. Voltage-gated proton channel is expressed on phagosomes. *Biochem Biophys Res Commun* 382: 274-279, 2009.
214. Pantazis A, Keegan P, Postma M, Schwiening CJ. The effect of neuronal morphology and membrane-permeant weak acid and base on the dissipation of depolarization-induced pH gradients in snail neurons. *Pflügers Arch* 452: 175-187, 2006.
215. Peterson E, Ryser T, Funk S, Inouye D, Sharma M, Qin H, Cross TA, Busath DD. Functional reconstitution of influenza A M2(22-62). *Biochim Biophys Acta* 1808: 516-521, 2011.
216. Petheő GL, Demaurex N. Voltage- and NADPH-dependence of electron currents generated by the phagocytic NADPH oxidase. *Biochem J* 388: 485-491, 2005.
217. Petheő GL, Orient A, Baráth M, Kovács I, Réthi B, Lányi A, Rajki A, Rajnavölgyi E, Geiszt M. Molecular and functional characterization of H_V1 proton channel in human granulocytes. *PLoS One* 5: e14081, 2010.
218. Pinto LH, Dieckmann GR, Gandhi CS, Papworth CG, Braman J, Shaughnessy MA, Lear JD, Lamb RA, DeGrado WF. A functionally defined model for the M2 proton channel of influenza A virus suggests a mechanism for its ion selectivity. *Proc Natl Acad Sci U S A* 94: 11301-11306, 1997.
219. Qiu ZH, Leslie CC. Protein kinase C-dependent and -independent pathways of mitogen-activated protein kinase activation in macrophages by stimuli that activate phospholipase A_2. *J Biol Chem* 269: 19480-19487, 1994.
220. de Quatrefages A. Observations sur les noctiluques. *Annales des Sciences Naturelles, Series 3, Zoologie* 14: 226-235, 1850.
221. Rada B, Lekstrom K, Damian S, Dupuy C, Leto TL. The *Pseudomonas* toxin pyocyanin inhibits the dual oxidase-based antimicrobial system as it imposes oxidative stress on airway epithelial cells. *J Immunol* 181: 4883-4893, 2008.
222. Rada BK, Geiszt M, Káldi K, Tímár C, Ligeti E. Dual role of phagocytic NADPH oxidase in bacterial killing. *Blood* 104: 2947-2953, 2004.
223. Ramsey IS, Mokrab Y, Carvacho I, Sands ZA, Sansom MSP, Clapham DE. An aqueous H^+ permeation pathway in the voltage-gated proton channel Hv1. *Nat Struct Mol Biol* 17: 869-875, 2010.
224. Ramsey IS, Moran MM, Chong JA, Clapham DE. A voltage-gated proton-selective channel lacking the pore domain. *Nature* 440: 1213-1216, 2006.
225. Ramsey IS, Ruchti E, Kaczmarek JS, Clapham DE. Hv1 proton channels are required for high-level NADPH oxidase-dependent superoxide production during the phagocyte respiratory burst. *Proc Natl Acad Sci U S A* 106: 7642-7647, 2009.
226. Reeves EP, Lu H, Jacobs HL, Messina CG, Bolsover S, Gabella G, Potma EO, Warley A, Roes J, Segal AW. Killing activity of neutrophils is mediated through activation of proteases by K^+ flux. *Nature* 416: 291-297, 2002.
227. Reth M, Dick TP. Voltage control for B cell activation. *Nat Immunol* 11: 191-192, 2010.
228. Roos A, Boron WF. Intracellular pH. *Physiol Rev* 61: 296-434, 1981.
229. Saaranen M, Suistomaa U, Kantola M, Saarikoski S, Vanha-Perttula T. Lead, magnesium, selenium and zinc in human seminal fluid: comparison with semen parameters and fertility. *Hum Reprod* 2: 475-479, 1987.
230. Sakata S, Kurokawa T, Norholm MH, Takagi M, Okochi Y, von Heijne G, Okamura Y. Functionality of the voltage-gated proton channel truncated in S4. *Proc Natl Acad Sci U S A* 107: 2313-2318, 2010.
231. Sánchez JC, Powell T, Staines HM, Wilkins RJ. Electrophysiological demonstration of voltage- activated H^+ channels in bovine articular chondrocytes. *Cell Physiol Biochem* 18: 85-90, 2006.
232. Sánchez JC, Wilkins RJ. Effects of hypotonic shock on intracellular pH in bovine articular chondrocytes. *Comp Biochem Physiol A Mol Integr Physiol* 135: 575-583, 2003.
233. Sansom MSP, Kerr ID, Smith GR, Son HS. The influenza A virus M2 channel: A molecular modeling and simulation study. *Virology* 233: 163-173, 1997.
234. Sasaki M, Takagi M, Okamura Y. A voltage sensor-domain protein is a voltage-gated proton channel. *Science* 312: 589-592, 2006.
235. Sbarra AJ, Karnovsky ML. The biochemical basis of phagocytosis. I. Metabolic changes during the ingestion of particles by polymorphonuclear leukocytes. *J Biol Chem* 234: 1355-1362, 1959.
236. Schilling T, Gratopp A, DeCoursey TE, Eder C. Voltage-activated proton currents in human lymphocytes. *J Physiol* 545: 93-105, 2002.
237. Schmitter RE, Njus D, Sulzman FM, Gooch VD, Hastings JW. Dinoflagellate bioluminescence: a comparative study of in vitro components. *J Cell Physiol* 87: 123-134, 1976.
238. Schowen RL. Solvent Isotope Effects on Enzymic Reactions. In: Cleland WW, O'Leary MH, Northrop DB, editors. *Isotope Effects on Enzyme-Catalyzed Reactions*, Baltimore: University Park Press, 1977, p. 64-99.
239. Schrenzel J, Lew DP, Krause KH. Proton currents in human eosinophils. *Am J Physiol* 271: C1861-C1871, 1996.
240. Schwarzer C, Machen TE, Illek B, Fischer H. NADPH oxidase-dependent acid production in airway epithelial cells. *J Biol Chem* 279: 36454-36461, 2004.
241. Schweighofer KJ, Pohorille A. Computer simulation of ion channel gating: The M_2 channel of influenza A virus in a lipid bilayer. *Biophys J* 78: 150-163, 2000.
242. Schwiening CJ, Willoughby D. Depolarization-induced pH microdomains and their relationship to calcium transients in isolated snail neurones. *J Physiol* 538: 371-382, 2002.
243. Seeds MC, Parce JW, Szejda P, Bass DA. Independent stimulation of membrane potential changes and the oxidative metabolic burst in polymorphonuclear leukocytes. *Blood* 65: 233-240, 1985.
244. Sesti F, Goldstein SA. Single-channel characteristics of wild-type I_{Ks} channels and channels formed with two minK mutants that cause long QT syndrome. *J Gen Physiol* 112: 651-663, 1998.
245. Sharma M, Yi M, Dong H, Qin H, Peterson E, Busath D, Zhou H, Cross T. Insight into the mechanism of the influenza A proton channel from structure in a lipid bilayer. *Science* 330: 509-512, 2010.
246. Sheldon C, Church J. Intracellular pH response to anoxia in acutely dissociated adult rat hippocampal CA1 neurons. *J. Neurophysiol* 87: 2209-2224, 2002.
247. Sheng J, Malkiel E, Katz J, Adolf JE, Place AR. A dinoflagellate exploits toxins to immobilize prey prior to ingestion. *Proc Natl Acad Sci U S A* 107: 2082-2087, 2010.
248. Shuck K, Lamb RA, Pinto LH. Analysis of the pore structure of the influenza A virus M_2 ion channel by the substituted-cysteine accessibility method. *J Virol* 74: 7755-7761, 2000.
249. Sklar LA, Jesaitis AJ, Painter RG, Cochrane CG. The kinetics of neutrophil activation. The response to chemotactic peptides depends upon whether ligand-receptor interaction is rate-limiting. *J Biol Chem* 256: 9909-9914, 1981.
250. Smith SME, Morgan D, Musset B, Cherny VV, Place AR, Hastings JW, DeCoursey TE. A novel voltage gated proton channel in a dinoflagellate. *Biophys J* 100: 284a. 2011
251. Smith SME, Morgan D, Musset B, Cherny VV, Place AR, Hastings JW, DeCoursey TE. Voltage-gated proton channel in a dinoflagellate. *Proc Natl Acad Sci U S A* 108: 18162-18168, 2011.
252. Smondyrev AM, Voth GA. Molecular dynamics simulation of proton transport near the surface of a phospholipid membrane. *Biophys J* 82: 1460-1468, 2002.
253. Starace DM, Stefani E, Bezanilla F. Voltage-dependent proton transport by the voltage sensor of the Shaker K^+ channel. *Neuron* 19: 1319-1327, 1997.
254. Szuszták K, Mócsai A, Ligeti E, Kapus A. Electrogenic H^+ pathway contributes to stimulus-induced changes of internal pH and membrane

potential in intact neutrophils: Role of cytoplasmic phospholipase A_2. *Biochem J* 325: 501-510, 1997.
255. Swenson ER, Deem S, Kerr ME, Bidani A. Inhibition of aquaporin-mediated CO_2 diffusion and voltage-gated H^+ channels by zinc does not alter rabbit lung CO_2 and NO excretion. *Clin Sci (Lond)* 103: 567-575, 2002.
256. Tajkhorshid E, Nollert P, Jensen MO, Miercke LJ, O'Connell J, Stroud RM, Schulten K. Control of the selectivity of the aquaporin water channel family by global orientational tuning. *Science* 296: 525-530, 2002.
257. Takanaka K, O'Brien PJ. Proton release associated with respiratory burst of polymorphonuclear leukocytes. *J Biochem* 103: 656-660, 1988.
258. Tao X, Lee A, Limapichat W, Dougherty DA, MacKinnon R. A gating charge transfer center in voltage sensors. *Science* 328: 67-73, 2010.
259. Taylor AR, Chrachri A, Wheeler G, Goddard H, Brownlee C. A voltage-gated H^+ channel underlying pH homeostasis in calcifying coccolithophores. *PLoS Biol* 9: e1001085, 2011.
260. Thomas RC, Meech RW. Hydrogen ion currents and intracellular pH in depolarized voltage-clamped snail neurones. *Nature* 299: 826-828, 1982.
261. Tombola F, Ulbrich MH, Isacoff EY. The voltage-gated proton channel Hv1 has two pores, each controlled by one voltage sensor. *Neuron* 58: 546-556, 2008.
262. Tombola F, Ulbrich MH, Kohout SC, Isacoff EY. The opening of the two pores of the Hv1 voltage-gated proton channel is tuned by cooperativity. *Nat Struct Mol Biol* 17: 44-50, 2010.
263. Turekian KK. *Oceans*: Prentice-Hall, Englewood Cliffs, N.J. 1968.
264. Urbach V, Helix N, Renaudon B, Harvey BJ. Cellular mechanisms for apical ATP effects on intracellular pH in human bronchial epithelium. *J Physiol* 543: 13-21, 2002.
265. van Zwieten R, Wever R, Hamers MN, Weening RS, Roos D. Extracellular proton release by stimulated neutrophils. *J Clin Invest* 68: 310-313, 1981.
266. Wang Y, Li SJ, Pan J, Che Y, Yin J, Zhao Q. Specific expression of the human voltage-gated proton channel Hv1 in highly metastatic breast cancer cells, promotes tumor progression and metastasis. *Biochem Biophys Res Commun* 412: 353-359, 2011.
267. Warner JA, MacGlashan DW, Jr. Signal transduction events in human basophils. A comparative study of the role of protein kinase C in basophils activated by anti-IgE antibody and formyl-methionyl-leucyl-phenylalanine. *J Immunol* 145: 1897-1905, 1990.
268. Whitin JC, Chapman CE, Simons ER, Chovaniec ME, Cohen HJ. Correlation between membrane potential changes and superoxide production in human granulocytes stimulated by phorbol myristate acetate. Evidence for defective activation in chronic granulomatous disease. *J Biol Chem* 255: 1874-1878, 1980.
269. Wikström M, Verkhovsky MI, Hummer G. Water-gated mechanism of proton translocation by cytochrome *c* oxidase. *Biochim Biophys Acta* 1604: 61-65, 2003.
270. Wood ML, Schow EV, Freites JA, White SH, Tombola F, Tobias DJ. Water wires in atomistic models of the Hv1 proton channel. *Biochim Biophys Acta*, 2011 doi:10.1016/j.bbamem.2011.07.045 [Epub ahead of print].
271. Woodward OM, Willows AO. Dopamine modulation of Ca^{2+} dependent Cl^- current regulates ciliary beat frequency controlling locomotion in *Tritonia diomedea*. *J Exp Biol* 209: 2749-2764, 2006.
272. Wraight CA. Chance and design–proton transfer in water, channels and bioenergetic proteins. *Biochim Biophys Acta* 1757: 886-912, 2006.
273. Wu B, Steinbronn C, Alsterfjord M, Zeuthen T, Beitz E. Concerted action of two cation filters in the aquaporin water channel. *Embo J* 28: 2188-2194, 2009.
274. Yamaguchi S, Miura C, Kikuchi K, Celino FT, Agusa T, Tanabe S, Miura T. Zinc is an essential trace element for spermatogenesis. *Proc Natl Acad Sci U S A* 106: 10859-10864, 2009.
275. Yang N, George AL, Jr, Horn R. Molecular basis of charge movement in voltage-gated sodium channels. *Neuron* 16: 113-122, 1996.
276. Yusaf SP, Wray D, Sivaprasadarao A. Measurement of the movement of the S4 segment during the activation of a voltage-gated potassium channel. *Pflügers Arch* 433: 91-97, 1996.

Further Reading

Reviews of voltage sensing mechanisms in ion channels:

1. Bezanilla F . The voltage sensor in voltage-dependent ion channels. *Physiol Rev* 80: 555-592, 2000.
2. Börjesson, SI, Elinder F. Structure, function, and modification of the voltage sensor in voltage-gated ion channels. *Cell Biochem Biophys* 52: 149-174, 2008.
3. Swartz KJ. Sensing voltage across lipid membranes. *Nature* 456: 891-897, 2008.
4. Tombola F, Pathak MM, Isacoff EY. How does voltage open an ion channel? *Annu Rev Cell Dev Biol* 22: 23-52, 2006.

A recent update on proposed functions of proton channels in various cells:

5. Capasso M, DeCoursey TE, Dyer MJS. pH regulation and beyond: Unanticipated functions for the voltage-gated proton channel, HVCN1. *Trends Cell Biol*. 21: 20-28, 2011.

This exhaustive review of voltage-gated proton channels includes comparisons with several other proton conducting molecules:

6. DeCoursey TE. Voltage-gated proton channels and other proton transfer pathways. *Physiol Rev* 83: 475-579, 2003.

A recent review of functions of proton channels in phagocytes:

7. Demaurex N, El Chemaly A. Physiological roles of voltage-gated proton channels in leukocytes. *J Physiol* 588: 4659-4665, 2010.

A recent focused review of functions of proton channels in sperm:

8. Kirichok, Y, Lishko PV. Rediscovering sperm ion channels with the patch-clamp technique. *Mol Hum Reprod* 17: 478-499, 2011.

A recent review of functions of proton channels in epithelium:

9. Fischer, H. Function of proton channels in lung epithelia. *WIRES Membr Transp Signal* (in press), 2011. doi: 10.1002/wmts.17

This is the classic textbook on ion channels:

10. Hille B. 2001. *Ion Channels of Excitable Membranes*. (3rd ed). Sunderland, MA: Sinauer Associates, Inc. p. 814.

Reviews of voltage-sensing phosphatases:

11. Okamura Y, Murata Y, Iwasaki H. Voltage-sensing phosphatase: Actions and potentials. *J Physiol* 587: 513-520, 2009.
12. Okamura Y. Biodiversity of voltage sensor domain proteins. *Pflügers Arch* 454: 361-371, 2007.